

ROBUST ITERATIVE LEARNING CONTROL DESIGN BASED ON GRADIENT METHOD

Shan Liu, Tiejun Wu

National Laboratory of Industrial Control Technology, Institute of Intelligent Systems and Decision Making, Zhejiang University, Hangzhou 310027, P.R. China

Abstract: An iterative learning control (ILC) method using both feedback and feedforward actions is proposed for a class of uncertain linear systems to achieve precise tracking control. A sufficient condition for the plant uncertainty and feedback controller, which guarantees the robust convergence of the learning, is given. The procedure of designing the robust algorithm has two steps: At first, the feedback controller with robust performance is synthesized based on H_∞ optimal approach according to the request of the sufficient condition; secondly, the incremental feedforward input signal is derived by gradient method with fixed step size. It is shown that the feedforward action has relation to the adjoint system of the closed nominal system. *Copyright © 2003 IFAC*

Keywords: Iterative learning control, H_∞ optimal control, gradient method, plant uncertainty.

1. INTRODUCTION

Iterative learning control (ILC) is a kind of feedforward control technique suitable to be applied systems or processes with repetitive operation in order to improve sequentially the control accuracy by performing the same task iteratively (Arimoto, *et al.*, 1984; Moore, 1998). While ILC has drawn continuous attention by its simplicity and tracking accuracy, most studies have been focused on the robustness of ILC schemes (Amann, *et al.*, 1996b; Furuta, *et al.*, 1987; Heinzinger, *et al.*, 1989; Moon, *et al.*, 1998; Padieu and Su, 1990). The initial robustness analysis concentrated on the open-loop ILC updating law (Heinzinger, *et al.*, 1989), but the purely open-loop ILC scheme may fail to work in practical applications because of the drawback that the tracking error may possibly grow quite large in the early stages of learning. Thus, the feedback controller is commonly employed along with the ILC to ensure the closed-loop stability. In this situation, the ILC algorithms designed for robustness against the original plant uncertainty are possibly unfit for the uncertainty of the closed-loop system.

Furuta, *et al.* (1987) derived a gradient-type ILC scheme by using a steepest-descent algorithm to minimize a performance criterion, but their approach is a pure feedforward type and consequently suffers from a lack of robustness in practice yet. Amman, *et al.* (1996a) proposed an ILC law using feedback and

feedforward actions on the basis of an optimization principle. Although their method has some degree robustness, it is unable to be applied to the plant with model uncertainty. Some researchers synthesize the ILC schemes based on the robust control theory. For example, Padieu, *et al.* (1990) presented general convergence conditions of ILC on the basis of H_∞ approach. Amann, *et al.* (1996b) showed a sufficient convergence condition for ILC with feedback controller and proposed a two-step design procedure based on H_∞ optimization. Moon, *et al.* (1998) reformulated the ILC design problem as a general robust control problem setup and gave a robust ILC procedure systematically. Most of the aforementioned approaches are designed and analyzed based on contraction mapping in frequency domain purely, but for any practical ILC process, a trial must end after a finite time. Thus, the conditions for convergence of these approaches can be overly restrictive because of the infinite time analysis of the feedforward action, sometimes leading to a requirement that the plant is invertible. For example, it is impossible to use general convergence condition in frequency domain for non-minimum-phase plants or strictly proper plants. Although a band-pass filter can be employed along with the feedforward action in order to relax the conservative convergence condition, the performance degradation that the tracking error will not converge to zero perfectly is caused in this case.

This paper focuses on the gradient-type ILC architecture of using both feedback and feedforward actions, and their performances are analyzed in the time domain and frequency domain respectively. A sufficient condition to guarantee the robust convergence of the learning strategy is given for a class of uncertain linear systems. Based on the derived sufficient condition, a two-step procedure of designing the robust ILC algorithm is proposed. First of all, the feedback controller with robust performance is synthesized based on H_∞ optimal approach according to the request of the sufficient condition; secondly, the incremental feedforward input signal is derived by gradient method with fixed step size.

This paper is organized as follows. Section 2 describes the ILC architecture with feedback controller and gives the relationship between original plant uncertainty and closed-loop system uncertainty. In section 3 a gradient-type ILC approach is proposed and a sufficient condition for robust convergence is derived in operator form. The design procedure based on H_∞ optimal approach and gradient method is presented in section 4. Section 5 verifies the usefulness of the proposed method through a simulation. Some concluding remarks are given in section 6.

2. ILC USING FEEDBACK AND FEEDFORWARD ACTIONS

Consider the controlled linear plant represented in operator form as

$$y = \tilde{P}u \quad (1)$$

where $u \in U$ and $y \in Y$, U and Y are a real Hilbert space with inner products $\langle \cdot, \cdot \rangle_u$ and $\langle \cdot, \cdot \rangle_y$

respectively. \tilde{P} is the system input-output operator, describing the dynamics of plants with unstructured uncertainties

$$\mathcal{P} = \{ \tilde{P} : \tilde{P} = P(I + \Delta_p W), \|\Delta_p\| \leq 1 \} \quad (2)$$

where P is the nominal plant operator, W is a fixed operator, Δ_p is a variable operator. Here $\|\cdot\|$ is the induced norm of operator.

Let $r(t)$ be a desired reference trajectory defined on the finite time interval $[0, T]$. An ILC system provides robustness against the plant uncertainty if it

provides convergence of the iterative process for every \tilde{P} in \mathcal{P} . It is equivalent to finding an ILC algorithm to construct a sequence of control inputs $\{u_k(t)\}$ converging to u_∞ as $k \rightarrow \infty$, such that u_∞ is the solution for the optimization problem

$$\min_u \{ J(u) = \|e\|_y^2 : e = r - y, y = \tilde{P}u \} \quad (3)$$

A block diagram of ILC using both feedback and feedforward actions is shown as Fig.1. In this figure, C is a feedback control operator and L is a feedforward control operator. The ILC approach in this case can be expressed as

$$\begin{cases} u_k = v_k - Cy_k \\ v_{k+1} = v_k + Le_k \end{cases} \quad (4)$$

where $e_k = r - y_k$ and v_k is feedforward input. In this scheme, the feedback controller ensures closed-loop stability and suppresses exogenous disturbances, and the feedforward controller provides improved tracking performance utilizing past control results.

The closed-loop operator from feedforward input v_k to system output y_k is easily given by

$$y_k = (I + \tilde{P}C)^{-1} \tilde{P}v_k = \tilde{P}(I + C\tilde{P})^{-1} v_k \quad (5)$$

The closed-loop operators corresponding to the uncertain system \tilde{P} and the nominal system P are represented by \tilde{G} and G , respectively. Hence, it yields

$$\tilde{G} = G(I + \Delta_p WCG)^{-1} (I + \Delta_p W) \quad (6)$$

From (6) it follows that

$$\begin{aligned} \tilde{G} = G & \left[I + (I + \Delta_p WCP(I + CP)^{-1})^{-1} \right. \\ & \left. \times \Delta_p W(I + CP)^{-1} \right] \end{aligned} \quad (7)$$

By defining the sensitivity and complementary sensitivity operators associated with the nominal system, i.e.,

$$S = (I + CP)^{-1}, T = CP(I + CP)^{-1} \quad (8)$$

and denoting the uncertainty of the closed-loop system by

$$\Delta_G = (I + \Delta_p WT)^{-1} \Delta_p WS \quad (9)$$

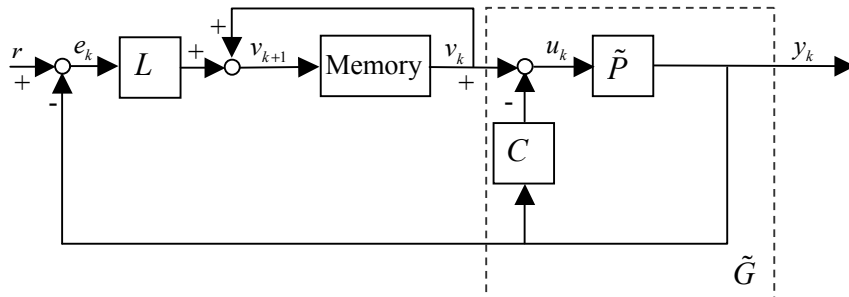


Fig.1. ILC using feedback and feedforward actions

the (7) can be rewritten as $\tilde{G} = G(I + \Delta_G)$. (9) implies the exact relationship between the uncertainty of the controlled system \tilde{P} and that of the closed-loop system \tilde{G} with feedback controller C .

3. ROBUST CONVERGENCE OF GRADIENT-TYPE ILC SCHEME

According to the aforementioned ILC configuration, if C as a fixed controller has already synthesized in advance to make the closed-loop system G of the nominal plant to achieve internal stable, the feedforward controller L can be designed based on the gradient method (Furuta, *et al.*, 1987). The gradient of J in (3) on v_k is

$$\Delta v_k = -G^* e_k \quad (10)$$

where G^* is the adjoint operator to G . Then the gradient-type ILC algorithm can be expressed as

$$v_{k+1} = v_k + \alpha G^* e_k \quad (11)$$

where α is a fixed step size of learning. For the actual closed-loop system \tilde{G} , by using the relation $e_k = r - \tilde{G}v_k$, from (11) it yields the error relation in the recursive form as

$$e_{k+1} = (I - \alpha \tilde{G}G^*) e_k \quad (12)$$

Hence

$$\begin{aligned} \|e_{k+1}\|_y^2 &= \|(I - \alpha \tilde{G}G^*) e_k\|_y^2 \\ &= \|e_k\|_y^2 + \alpha^2 \|\tilde{G}G^* e_k\|_y^2 - 2\alpha \langle e_k, \tilde{G}G^* e_k \rangle_y \end{aligned} \quad (13)$$

which leads to, by using the property of induced norm and the Schwarz inequality,

$$\begin{aligned} \|e_{k+1}\|_y^2 - \|e_k\|_y^2 &= \alpha^2 \|\tilde{G}G^* e_k\|_y^2 - 2\alpha \|G^* e_k\|_u^2 \\ &\quad - 2\alpha \langle G^* e_k, \Delta_G G^* e_k \rangle_u \\ &\leq \alpha \left(\alpha \|\tilde{G}\|^2 + 2\|\Delta_G\| - 2 \right) \|G^* e_k\|_u^2 \end{aligned} \quad (14)$$

Note that if $\|\Delta_G\| \leq \infty$, then $\|\tilde{G}\| \leq \|G\|(1 + \|\Delta_G\|) \leq \infty$. From (14), a sufficient condition can be obtained to ensure that the error sequence $\{\|e_k\|_y\}$ is monotonically non-increasing in k is

$$\alpha \|\tilde{G}\|^2 + 2\|\Delta_G\| - 2 < 0 \quad (15)$$

In view of the fact that (15) gives $\|\Delta_G\| < 1 - \frac{1}{2} \alpha \|\tilde{G}\|^2$, due to the step size $\alpha > 0$, the above sufficient condition implies that $\|\Delta_G\| \leq \delta < 1$, where δ is a positive number. Thus, in order to ensure the robust convergence of the ILC law (11), the step size α need to be chosen in the range defined in the following

$$0 < \alpha < \frac{2 - 2\delta}{\|G\|^2 (1 + \delta)^2} \quad (16)$$

As a result, from (14), (15) and (16) it follows that

$$\begin{aligned} \|e_{k+1}\|_y^2 - \|e_k\|_y^2 \\ \leq \alpha \left[\alpha \|G\|^2 (1 + \delta)^2 + 2\delta - 2 \right] \|G^* e_k\|_u^2 \leq 0 \end{aligned}$$

Thus the ILC law (11) is convergent for every plant satisfying the condition $\|\Delta_G\| \leq \delta < 1$.

If δ is much close to 1, however, the condition (16) will become very strict and conservative, i.e., the step size α has to be chosen much small and, as a result, the convergence speed will be very slow.

The following theorem shows that the condition of choosing step size can be relaxed while the robustness for convergence of the ILC process will be maintained in the presence of plant uncertainty.

Theorem 1. Assume a set of uncertain systems as

$$\{\tilde{G} : \tilde{G} = G(I + \Delta_G), \|G\| < \infty, \|\Delta_G\| \leq \delta < 1\} \quad (17)$$

and the ILC updating law is given by (11). If the learning step size α satisfies

$$0 < \alpha \leq \frac{1}{\|G\|^2} \quad (18)$$

then for every plant \tilde{G} satisfying (17),

1) the ILC tracking error sequence $\{e_k\}$ converges to a limited e_∞ when $k \rightarrow \infty$;

2) the ILC tracking error sequence $\{e_k\}$ converges to zero if $\ker(G^*) = 0$.

Proof:

Substituting condition (17) into (13) yields

$$\begin{aligned} \|e_{k+1}\|_y^2 - \|e_k\|_y^2 &= \alpha^2 \|G(I + \Delta_G)G^* e_k\|_y^2 \\ &\quad - 2\alpha \langle e_k, GG^* e_k \rangle_y - 2\alpha \langle e_k, G\Delta_G G^* e_k \rangle_y \\ &= \alpha^2 \left(\|GG^* e_k\|_y^2 + \|G\Delta_G G^* e_k\|_y^2 \right. \\ &\quad \left. + \langle (\Delta_G^* G^* G + G^* G\Delta_G)G^* e_k, G^* e_k \rangle_u \right) \\ &\quad - \alpha \left(2\|G^* e_k\|_u^2 + \langle (\Delta_G^* + \Delta_G)G^* e_k, G^* e_k \rangle_u \right) \\ &= \alpha \left\langle \left(\alpha (G^* G + \Delta_G^* G^* G\Delta_G + \Delta_G^* G^* G \right. \right. \\ &\quad \left. \left. + G^* G\Delta_G) - 2I - (\Delta_G^* + \Delta_G) \right) G^* e_k, G^* e_k \right\rangle_u \end{aligned} \quad (19)$$

In view of the fact that

$$\begin{aligned} &\alpha (G^* G + \Delta_G^* G^* G\Delta_G + \Delta_G^* G^* G + G^* G\Delta_G) \\ &\quad - 2I - (\Delta_G^* + \Delta_G) \\ &= (I + \Delta_G^*) \left[(\alpha G^* G - I) + (\alpha G^* G\Delta_G - I) \right] \\ &\quad + \Delta_G^* - \Delta_G \\ &= (I + \Delta_G^*) \left[(\alpha G^* G - I)(I + \Delta_G) + (\Delta_G - I) \right] \\ &\quad + \Delta_G^* - \Delta_G \\ &= (I + \Delta_G^*) (\alpha G^* G - I)(I + \Delta_G) \\ &\quad + (I + \Delta_G^*) (\Delta_G - I) + \Delta_G^* - \Delta_G \\ &= (I + \Delta_G^*) (\alpha G^* G - I)(I + \Delta_G) + \Delta_G^* \Delta_G - I \end{aligned} \quad (20)$$

using the property that $\|G\|^2 = \|G^*\|^2 = \|G^* G\|$ and (18) we obtain

$$\|\alpha G^* G\| \leq 1 \quad (21)$$

Thus $(I + \Delta_G^*)(\alpha G^* G - I)(I + \Delta_G)$ is a non-positive definite self-adjoint operator. From the system uncertainty condition (17), $\|\Delta_G\| \leq \delta < 1$, it follows that $\Delta_G^* \Delta_G - I$ is a negative definite self-adjoint operator. Note that $\alpha > 0$, hence

$$\|e_{k+1}\|_y^2 - \|e_k\|_y^2 < \alpha(\delta^2 - 1)\|G^* e_k\|_u^2 \leq 0 \quad (22)$$

Thus the sequence $\{\|e_k\|_y^2\}$ is monotonically non-increasing and converges to a limited limit, and $\lim_{k \rightarrow \infty} \|e_{k+1}\|_y^2 - \|e_k\|_y^2 = 0$. Then let $k \rightarrow \infty$ in (22), it can be concluded that

$$0 \leq \alpha(\delta^2 - 1) \lim_{k \rightarrow \infty} \|G^* e_k\|_u^2 \leq 0 \quad (23)$$

i.e., $\lim_{k \rightarrow \infty} \|G^* e_k\|_u = 0$, or, equivalently, $\lim_{k \rightarrow \infty} G^* e_k = 0$.

If the nominal plant satisfies $\ker(G^*) = 0$, there exists no non-zero e such that $G^* e = 0$, and it follows that $\lim_{k \rightarrow \infty} e_k = 0$. ■

Remark 1. From a result of the operator theory, i.e., $\overline{\mathfrak{R}(G)} = [\ker(G^*)]^\perp$, where \mathfrak{R} denotes the range of an operator and $\overline{\mathfrak{R}(G)}$ the closure of $\mathfrak{R}(G)$, it follows that $\ker(G^*) = 0$ implies $Y = \mathfrak{R}(G)$ or $\mathfrak{R}(G)$ is dense in Y (Amann, *et al.*, 1996a). Hence, the condition $\ker(G^*) = 0$ means that for any desired output trajectory r , there exists input u_d that drives the nominal plant to produce the output $y = r$. This condition can be weakened to that the desired output trajectory $r \in \mathfrak{R}(G)$ or $r \in \overline{\mathfrak{R}(G)}$, which implies the given desired output trajectory can be tracked exactly by the nominal plant output. These are the reasonable assumptions usually made in ILC studies.

Remark 2. The condition (17) in theorem 1 is not only a sufficient condition for the gradient-type ILC process to converge but also a condition for synthesizing the feedback controller C .

It is worthwhile to point out that theorem 1 can not directly applicable to the design of controller C , because the plant uncertainty and controller C are implicitly involved in the sufficient condition (17). The following theorem gives a realizable solution for designing the feedback controller C .

Theorem 2. Suppose the uncertain system \tilde{P} described as (1) and (2), and the ILC updating law is given by (11) and (18). If the condition

$$\|WT\| + \|WS\| < 1 \quad (24)$$

is satisfied, then the ILC system is convergent.

Proof:

From theorem 1 and (9), a sufficient condition for the ILC to converge is $\|(I + \Delta_p WT)^{-1} \Delta_p WS\| < 1$. Note that

$$\begin{aligned} & \|(I + \Delta_p WT)^{-1} \Delta_p WS\| \\ & < \|(I + \Delta_p WT)^{-1}\| \|\Delta_p\| \|WS\| \end{aligned} \quad (25)$$

Because of the fact that (24) implies $\|WT\| < 1$, from $\|\Delta_p\| \leq 1$ we have $\|\Delta_p WT\| \leq \|\Delta_p\| \|WT\| < 1$. Therefore,

$$\|(I + \Delta_p WT)^{-1}\| < \frac{1}{1 - \|\Delta_p WT\|} < \frac{1}{1 - \|WT\|} \quad (26)$$

Combining (25) and condition (24) yields

$$\|(I + \Delta_p WT)^{-1} \Delta_p WS\| < \frac{\|WS\|}{1 - \|WT\|} < 1 \quad (27)$$

Hence the ILC system is convergent. ■

Remark 3. Note that condition (24) has the similar form as the robust performance condition for the uncertain plant \tilde{P} and the controller C . Thus theorem 2 has shown that the robust ILC system for the uncertain plant can be designed in two steps: At first, synthesize the feedback controller achieving robust performance according to the condition (24) independently; secondly, design the feedforward controller based on the gradient method.

Remark 4. Due to the fact that

$$\|W\| = \|W(S + T)\| \leq \|WS\| + \|WT\|$$

a necessary condition for (24) is $\|W\| < 1$.

4. ROBUST ILC ALGORITHM BASED ON H_∞ OPTIMAL APPROACH

The aforementioned analysis is established in the general linear operator space. The practical computational algorithm depends on the form of systems dynamics in detail.

Suppose input space U is $L_2^m[0, T]$ and output space Y is $L_2^n[0, T]$, the inner products in U and Y are defined as

$$\langle u_1, u_2 \rangle_u = \langle u_1, u_2 \rangle_{2T} = \int_0^T u_1^T(t) u_2(t) dt$$

$$\langle y_1, y_2 \rangle_y = \langle y_1, y_2 \rangle_{2T} = \int_0^T y_1^T(t) y_2(t) dt$$

the induced norm of plant P is denoted $\|P\|$. In the meantime, suppose the extended input space \bar{U} is $L_2^m[0, +\infty)$ and the extended output space \bar{Y} is $L_2^n[0, +\infty)$, the inner products in \bar{U} and \bar{Y} are defined as

$$\langle u_1, u_2 \rangle_{\bar{u}} = \langle u_1, u_2 \rangle_{\bar{2}} = \int_0^{+\infty} u_1^T(t) u_2(t) dt$$

$$\langle y_1, y_2 \rangle_{\bar{y}} = \langle y_1, y_2 \rangle_{\bar{2}} = \int_0^{+\infty} y_1^T(t) y_2(t) dt$$

the extended induced norm of plant P is denoted $\|P\|_\infty$, i.e., H_∞ norm. The following lemma shows the relationship between $\|P\|_\infty$ and $\|P\|$.

Lemma 1. Consider the plant P as either an operator from $L_2^m[0, T]$ to $L_2^n[0, T]$, or an operator from $L_2^m[0, +\infty)$ to $L_2^n[0, +\infty)$. The corresponding induced norm and the extended induced norm of P

are $\|P\|$ and $\|P\|_\infty$, respectively, then

$$\|P\| \leq \|P\|_\infty \quad (28)$$

The following theorem is derived from lemma 1 and theorem 2 immediately.

Theorem 3. Consider the uncertain system \tilde{P} described as (1) and (2), regarded as an operator from $L_2^m[0, T]$ to $L_2^n[0, T]$. The ILC updating law is described as (11) and (18). If the condition

$$\|WT\|_\infty + \|WS\|_\infty < 1 \quad (29)$$

is satisfied, then the ILC system is convergent.

It has been clearly shown from (29) that a more conservative sufficient condition ensuring the ILC robustly converge is $\|WT\|_\infty < \frac{1}{2}$ and $\|WS\|_\infty < \frac{1}{2}$, or

$$\left\| \begin{bmatrix} WS \\ WT \end{bmatrix} \right\|_\infty < \frac{1}{2} \quad (30)$$

Hence, the feedback controller C can be obtained by H_∞ optimal approach. According to the linear fractional transformation (LFT) and

$$\begin{bmatrix} WS \\ WT \end{bmatrix} = \begin{bmatrix} W \\ 0 \end{bmatrix} + \begin{bmatrix} -W \\ W \end{bmatrix} C(I+PC)^{-1}P \quad (31)$$

the "augmented plant" P_H in the standard H_∞ control problem is

$$P_H = \begin{bmatrix} W & -W \\ 0 & W \\ P & -P \end{bmatrix} \quad (32)$$

On the other hand, for linear system, if the feedback controller C is given, the adjoint system of the closed-loop system G can be synthesized directly. Suppose that G has m inputs and n outputs with dynamics described by a linear continuous state-space form as

$$\left. \begin{aligned} \dot{x}(t) &= A(t)x(t) + B(t)u(t) \\ y(t) &= C(t)x(t) \end{aligned} \right\} \quad (33)$$

where $x(t)$, $u(t)$ and $y(t)$ represent the state, the input and the output, respectively. The initial state of system is

$$x(t_0) = x_0 \quad (34)$$

In this case, the adjoint system G^* of system G can be obtained by

$$\left. \begin{aligned} \dot{g}(t) &= -A^T(t)g(t) - C^T(t)w(t) \\ z(t) &= B^T(t)g(t) \end{aligned} \right\} \quad (35)$$

the corresponding terminal boundary condition of G^* is relation to practical performance index. For example, the terminal boundary condition corresponding to performance index (3) is

$$g(T) = 0 \quad (36)$$

The computational procedure for robust ILC algorithm based on the H_∞ optimal approach and the gradient method is summarized as follows:

1) For the uncertain system \tilde{P} described as (1) and (2), design the feedback controller C by solving the conventional H_∞ optimal control problem (Zhou, *et*

al., 1996) according to the augmented plant (32), and examine the condition (29) and (30).

2) Fix the feedback controller C . Get the closed-loop system G of the nominal plant P and transform G to its minimal realization as (33) and (34), then solve the adjoint system G^* of G according to (35) and (36).

3) Get the ILC updating law according to (11) and (18).

5. SIMULATION EXAMPLE

To illustrate the robustness of the algorithm, the simulation results for the same plant used by Moon, *et al.* (1998) is given in this section. The nominal plant and the uncertainty weighting function are

$$P(s) = \frac{25s+80}{s^2+24s+370}, \quad W(s) = 0.5 \frac{s+10}{s+100}$$

where $|W(s)|$ is an increasing function of frequency,

the initial state is $x(0) = 0$. The uncertain system model is described as (2). The reference trajectory to be tracked contains frequency components of up to 8 Hz and is composed of a series of harmonious sinusoidal signals, i.e.,

$$r(t) = 4 \sin(2\pi t) + \sin(4\pi t) + 0.75 \sin(8\pi t) + 0.5 \sin(16\pi t)$$

where $t \in [0, 1]$.

Following the design procedure in Section 4, according to (28) the H_∞ augmented plant is

$$G_H(s) = \begin{bmatrix} 0.5 \frac{s+10}{s+100} & -0.5 \frac{s+10}{s+100} \\ 0 & 0.5 \frac{s+10}{s+100} \\ \frac{25s+80}{s^2+24s+370} & -\frac{25s+80}{s^2+24s+370} \end{bmatrix}$$

The feedback controller C was obtained by solving the conventional H_∞ optimal control approach, i.e.,

$$A_c = \begin{bmatrix} -6.9 & 3.1 & -10.4 & -0.8 \\ -32.7 & -112.4 & -156.7 & -29.2 \\ -159.4 & -21 & -523.3 & -61.2 \\ -376.6 & 38.5 & -1131 & -210.5 \end{bmatrix},$$

$$B_c = [4.369 \quad -32.82 \quad -183 \quad -423.8]^T,$$

$$C_c = [-0.6046 \quad 3.482 \quad 2.406 \quad 2.591],$$

$$D_c = [0]$$

In this case, $\left\| \begin{bmatrix} WS \\ WT \end{bmatrix} \right\|_\infty < 0.5039$, which does not satisfy the condition (30). Notice the fact that $\|WS\|_\infty = 0.5006$ and $\|WT\|_\infty = 0.2782$, however, we have $\|WS\|_\infty + \|WT\|_\infty = 0.7788 < 1$. It satisfies the condition (29), this shows that the algorithm proposed in this paper is applicable to the uncertain system in this example.

We applied the ILC updating law obtained from the design procedure to three representative plants in the set of uncertain systems for comparison:

Plant 1. $\Delta_p = 1.0$

Plant 2. $\Delta_p = 0$ (the nominal plant)

Plant 3. $\Delta_p = -1.0$

Fig. 2 shows the tracking output of the plant 1 for 40 iterations. Fig. 3 shows the root mean square (rms) values of the tracking error versus the iteration numbers. It is clearly seen the algorithm converges in similar speed for those representative plants. This indicates the robustness of the proposed algorithm against the plant uncertainty.

Compare the tracking control performances of the proposed algorithm with those of Moon's learning algorithm in (Moon, *et al.*, 1998). While the simulation result in (Moon, *et al.*, 1998) shows that the tracking error converges after 10th trial and the rms value of the ultimate error is about 0.5, the simulation results of the proposed algorithm show that the tracking error seems to converge after the 40th trial and the rms value of the ultimate error is less than 0.1 for every representative plant. It can be observed from fig. 3 that the rms value of the tracking error is less than 0.32 after 10th trail. This verifies the benefit of the proposed algorithm.

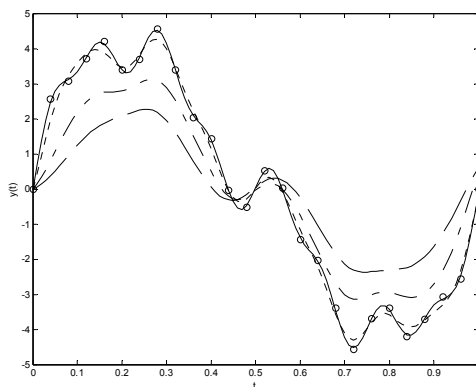


Fig. 2. Output and reference of the plant 1

Legend: dashed line (---) trail 1; dashdot line (-.-) trail 2; dotted line (···) trail 10; solid line (—) trail 40; "o" reference

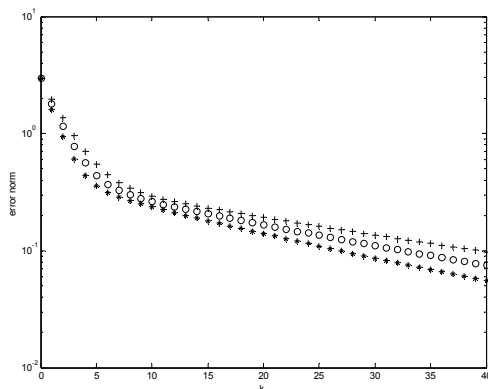


Fig. 3. RMS values of tracking errors versus iteration number

Legend: "+" $\Delta_p = -1.0$; "o" $\Delta_p = 0$; "*" $\Delta_p = 1.0$

6. CONCLUSIONS

In this paper, a gradient-type ILC design method using both feedback and feedforward actions is proposed for a class of uncertain linear systems. In order to avoid the drawback of the ILC method designed in frequency domain purely that the convergence analysis is made in the infinite time range, a sufficient condition for convergence of the iterative process in the presence of plant uncertainty is derived from the operator theory. The feedforward action is obtained by the gradient method and the feedback action is synthesized by the standard H_∞ optimal approach. Based on the derived sufficient condition, a two-step procedure of designing the robust ILC algorithm is suggested. It is shown that the feedforward action has relation to the adjoint system of the closed nominal system. The simulation result demonstrates the effectiveness and robustness of the proposed ILC algorithm against the plant uncertainty.

REFERENCES

- Amann N., D. H. Owens and E. Rogers (1996a). Iterative learning control using optimal feedback and feedforward actions. *International Journal of Control*, **65**(2), 277-293.
- Amann N., D. H. Owens, E. Rogers and A. Wahl (1996b). An H_∞ approach to linear iterative learning control design. *International Journal of Adaptive Control and Signal Processing*, **10**(6), 767-781.
- Arimoto, S., S. Kawamura and F. Miyazaki (1984). Bettering operation of robots by learning. *Journal of Robotic Systems*, **1**(2), 123-140.
- Furuta, K. and M. Yamakita (1987). The design of a learning control system for multivariable systems. In: *Proceedings of the 1987 IEEE International Symposium on Intelligent Control*, 371-376, Philadelphia, Pennsylvania, USA.
- Heinzinger G., D. Fenwick, B. Paden and F. Miyazaki (1989). Robust learning control. In: *Proceedings of the 28th IEEE Conference on Decision and Control*, 436-440, Tampa, FL.
- Moon J. H., T. Y. Doh, and M. J. Chung (1998). A robust approach to iterative learning control design for uncertain systems. *Automatica*, **34**(8), 1001-1004.
- Moore, K. L. (1998). Iterative learning control - an expository overview. *Applied and Computational Controls, Signal Processing and Circuits*, **1**, 151-214.
- Padieu F. and R. Su (1990). An H_∞ approach to learning control system. *International Journal of Adaptive Control and Signal Processing*, **4**, 465-474.
- Zhou, K., J. C. Doyle and K. Glover (1996). *Robust and Optimal Control*. Prentice-Hall, Englewood Cliffs.

COMPENSATOR FOR INTERNET-BASED ADVANCED CONTROL

X Chen and S H Yang*

*Computer Science Department, Loughborough University, Loughborough, Leicestershire
LE11 3TU UK
Telephone: 0044 1509 222942, Fax: 0044 1509 211586,
Email: s.h.yang@lboro.ac.uk*

Abstract: Internet-based control is becoming next generations of control systems, in which time delay and data loss in Internet transmission are the major obstacles for bringing this control system into a reality. This paper proposes new control architecture in cooperated with two compensators to attack this major difficulty. These two compensators are located in the feedback and feed-forward channels in the architecture in order to compensate the control action and assure the stability of the control system. The novel compensators and control system architecture are illustrated and evaluated through a simulation example by using the DMC control algorithm. *Copyright © 2002 IFAC*

Keywords: Process control; predictive control; time delay; data transmission.

1. INTRODUCTION

In past years, the success to adopt the Internet to deliver business services has demonstrated a lot of advantages, such as cost reduction, flexibility. In the control area, researchers begin to exploit the advantages of the Internet for control systems, namely Internet-based control system. Such control systems are characterised as globally remote monitoring and adjustment of plants over the Internet. With the prevalence of the Internet, plants stand to benefit from the ways of retrieving data and reacting to plant fluctuations from anywhere around the world at any time. From higher education institutions, researchers have developed web-based virtual control laboratories for distance learning purposes (Shaheen, et al., 1998; Overstreet and Tzes, 1999). Some small-scale demonstrators of Internet-based control have implemented and shown a number of promising results (Yang, et al., 2002a; Halley and Gauld, 1999). Meanwhile, a few companies are more likely to produce Internet-based control systems as a control device (Cushing, 2000). The first systematic design method of Internet-based control systems has been formalised in our recent work (Yang, et al., 2003).

The Internet-based control systems, which have been achieved so far, adopt a discrete control structure, which do not explicitly consider Internet transmission features. For example, Overstreet and Tzes (1999) inserted Internet communication elements between the remote controller and the sampling switches in their Internet-based laboratory control system. They directly adopted a discrete control structure and treated the Internet transmission as a pure lag element. As described in the following section, Internet time delay is determined by the Internet circumstances such as the amount of transmission data, the connection bandwidth, and the distance between the sending and receiving nodes. Therefore Internet time delay cannot be modelled and predicted. Data loss is another significant issue and has a great influence on the performance of control systems.

Therefore, it is essential to study the features of the Internet transmission, and propose a proper measure to overcome the Internet time delay and data loss for Internet-based control systems. This study is organised as follows: Section 2 describes the features of Internet transmission. Section 3 gives out a control structure with a tolerant period of time for sampling. Two compensators located at the feedback and feed-

*To whom correspondence should be addressed.

forward channels are designed in Section 4 to fully exploit the benefit of the control architecture. A simulation study is used to assess the performance of the compensators in Section 5. Section 6 is the conclusion.

2. INTERNET TRANSMISSION LATENCY

The Internet is a public transmission media, which is fundamentally different from other private transmission medias used by many end-users for different purposes. The exiting studies of the Internet transmission (Luo and Chen, 2000; Acharya and Saltz, 1996) show that the performance associated with time-delay and data-loss possesses large temporal and spatial variation, and uncertain transmitting time-delay and data-loss problems are not avoidable for any Internet-based application.

In detail, the Internet time delay is characterized by the processing speed of nodes, the load of nodes, the connection bandwidth, the amount of data, the transmission speed, etc. The Internet time delay $T_d(k)$ at instant k can be described as follows:

$$\begin{aligned} T_d(k) &= \sum_{i=0}^n \left[\frac{l_i}{C} + t_i^R + t_i^L(k) + \frac{M}{b_i} \right] \\ &= \sum_{i=0}^n \left(\frac{l_i}{C} + t_i^R + \frac{M}{b_i} \right) + \sum_{i=0}^n t_i^L(k) \\ &= d_N + d_L(k) \end{aligned} \quad (1)$$

where l_i is the i th length of link, C the speed of light, t_i^R the routing speed of the i th node, $t_i^L(k)$ the delay caused by the i th node's load, M the amount of data, and b_i the bandwidth of the i th link. d_N is a term, which is independent of time, and $d_L(k)$ is a time-dependent term. Because of the time-dependent term $d_L(k)$ it is somewhat unreasonable to model the Internet time delay for accurate prediction at every instant.

Therefore the performance of the Internet transmission cannot be modelled and predicted, which is necessary to be explicitly handled by control systems.

3. INTERNET-BASED CONTROL ARCHITECTURE

It is arguable that the conventional discrete control structure, which uses a fixed sampling interval, is not suitable for Internet-based control systems. The discrete control structure requires a predictable execution time for closed control loops. Conversely, Internet transmission time delay is unpredictable, which breaks the foundation of the conventional discrete control structure. For example, an actuator may receive a control signal from a controller after the sampling interval passes. As the result, the control system may lose a number of control signals because of the fixed sampling interval. Therefore, a suitable control structure is required to deal with the

uncertain execution time, time delay, and data loss for Internet-based control systems.

Conceptually, the architecture should involve several network services and a control functional structure. This paper only addresses the control functional structure. The network services such as global timers and real time control protocols can be referred to our recent work (Chen and Yang, 2002). The evolvement of the Internet-based control functional structure is shown in Fig 1, which maintains the main function of the structure, such as Zero-Order Hold (ZOH). If the discrete control structure (the above part in Fig 1) is considered as a tight coupling structure, the new structure (the lower part in Fig 1) is a loose coupling structure, which introduces a tolerance time Δt to handle the unpredictable Internet communication. The tolerance time chosen must be shorter than the sampling interval, so that the control law can still be maintained. Rather than transmitting control signals at a series of fixed time points, the new structure transmits control signals within a series of time intervals, which theoretically maximises the opportunity for control signals being transmitted on time. In order to implement the new structure, the sampling switches in the conventional discrete control structure is replaced with a pair of sampling switches located in both remote and local sides. The timers synchronised by the network service trigger the sampling switches.

Another significant feature introduced here in the Internet based control structure is that a signal buffer is employed at the feedback channel (see the lower part in Fig 1). The control command becomes useless after an unexpected long time delay, which is treated as a noise. In contrast, the delayed feedback signal is still useful, particularly for updating predictive models for processes. In the Internet based control structure the time-out control command signals are omitted and the delivery of the feedback signal is guaranteed.

4. DEALING WITH TIME DELAY AND DATA LOSS IN CONTROL SYSTEM DESIGN

Although the new control structure is well designed to cope with the Internet features, the traditional controller cannot fully take the advantage of the control structure. It is necessary to add-on some functional elements to efficiently use the new structure. Two compensators for a predictive controller have been designed, which are located at the feedback and feed-forward channels respectively. The widely accepted predictive controller, Dynamic Matrix Controller (DMC), has been chosen to integrate with these two compensators and demonstrate the novel architecture. The concept is shown in Fig 2. The compensator at the feedback channel with a data buffer located at the local side is designed to overcome time delay and data loss occurring in the transmission from the local side to a

remote side. The compensator at the feed-forward channel is designed to overcome time delay and data

loss occurring in the transmission from a remote side to the local side.

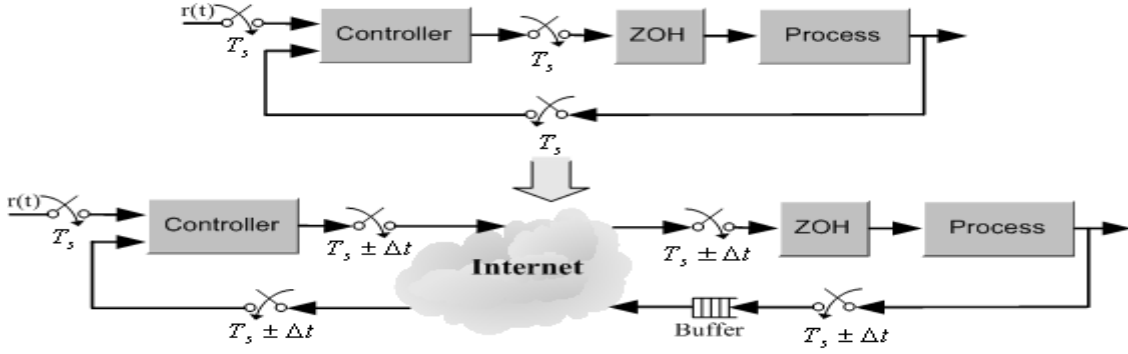


Fig. 1. Evolution of the control structure

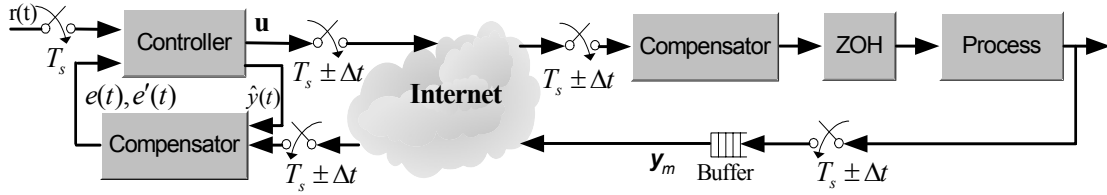


Fig. 2. Predictive controller with data loss and time delay compensators.

4.1 Dynamic Matrix Controller (DMC)

DMC was developed at the end of the seventies by Cutler and Ramaker (1980) of Shell Oil Co. and has been widely accepted in the industrial world, mainly by petrochemical industries. DMC can be divided into prediction and control law two parts.

The process model employed in the DMC formulation is a step response of the plant as shown in Equation 2, while the disturbance is considered to keep constant along the horizon. The procedure of obtaining the predictions is reviewed from Equations 2 to 5 as follows:

$$y(t) = \sum_{i=1}^{\infty} g_i \Delta u(t-i) \quad (2)$$

where $y(t)$ is the output of the process, g_i is the sampled output value for the step input, Δu is the control action. Denote $f(t+k)$ as the free response of the system, that is, the part of the response that does not depend on the future control actions. For the asymptotically stable process, the coefficients g_i of the step response tends to be a constant value after N sampling periods. The free response can be given as:

$$f(t+k) = y_m(t) + \sum_{i=1}^N (g_{k+i} - g_i) \Delta u(t-i) \quad (3)$$

Now the predictions can be computed along the prediction horizon ($k=1, \dots, p$), considering m control actions.

defining the input vector composed of the future control increments $\Delta \mathbf{u}$ as:

$$\Delta \mathbf{u} = [\Delta u(t) \quad \Delta u(t+1) \quad \dots \quad \Delta u(t+m-2) \quad \Delta u(t+m-1)]^T$$

defining the estimates of output vector \mathbf{y} as:

$$\hat{\mathbf{y}} = [\hat{y}(t+1|t) \quad \hat{y}(t+2|t) \quad \dots \quad \hat{y}(t+p-1|t) \quad \hat{y}(t+p|t)]^T$$

defining the system's dynamic matrix \mathbf{G} as:

$$\mathbf{G} = \begin{bmatrix} g_1 & 0 & \dots & 0 & 0 \\ g_2 & g_1 & 0 & \dots & 0 \\ \vdots & \vdots & \ddots & & \vdots \\ g_m & g_{m-1} & \dots & g_2 & g_1 \\ \vdots & \vdots & \ddots & \vdots & \vdots \\ g_p & g_{p-1} & \dots & g_{p-m+2} & g_{p-m+1} \end{bmatrix}_{p \times m} \quad (4)$$

defining the free response vector \mathbf{f} as:

$$\mathbf{f} = [f(t+1) \quad f(t+2) \quad \dots \quad f(t+p-1) \quad f(t+p)]^T$$

T means the transfer of the vector. Then the prediction equation can be written as:

$$\hat{\mathbf{y}} = \mathbf{G} \Delta \mathbf{u} + \mathbf{f} \quad (5)$$

The objective of a DMC controller is to drive the output as close to the setpoint as possible in a least-squares sense with the possibility of the inclusion of a penalty term on the input moves. Therefore, the general results of the control law can be given as:

$$\Delta \mathbf{u} = (\mathbf{G}^T \mathbf{G} + \lambda \mathbf{I})^{-1} \mathbf{G}^T (\mathbf{w} - \mathbf{f}) \quad (6)$$

\mathbf{w} is reference trajectory vector. The elements of \mathbf{w} are represented as:

$$\begin{cases} w(t) = y_m(t) \\ w(t+k) = \alpha w(t+k-1) + (1-\alpha)r(t+k) \\ k = 1, \dots, N \end{cases} \quad (7)$$

α is a parameter between 0 and 1.

4.2 Compensator at the feedback channel

The objective of the compensator at the feedback channel is to reduce the effect of time delay and data loss occurring in the feedback channel, i.e. the feedback signal compression, by means of the history data stored at the buffer. It is required to separate the

feedback signal from the control action in order to compensate the influence purely at the feedback channel.

In the prediction (Equation 5) only \mathbf{f} involves the feedback signal. Equation 3 is rewritten as:

$$f(t+k) = \hat{y}(t|t) + e(t) + \sum_{i=1}^N (g_{k+i} - g_i) \Delta u(t-i) \quad (8)$$

where $e(t)$ is the adjustment value of the prediction model associated with the feedback, and is defined as:

$$e(t) = \beta(y_m(t) - \hat{y}(t|t)) \quad (9)$$

β is a parameter between 0 and 1 to adjust the effect of the feedback value. If β is 1, Equations 3 and 8 become identical.

In the control law (Equations 6 and 7), $w(t)$ includes the feedback signals and can be rewritten as:

$$w(t) = \hat{y}(t|t) + e'(t) \quad (10)$$

where $e'(t) = y_m(t) - \hat{y}(t|t)$

When the data loss occurs and/or the feedback signals do not arrive on time because of the time delay, it is assumed that the prediction value is equal to the measured value, then $e(t)$ and $e'(t)$ in Equations 8 and 10 can be set to zero. The control actions purely rely on the model prediction. Therefore, Equations 8 and 10 become:

$$\begin{aligned} f'(t+k) &= \hat{y}(t|t) + \sum_{i=1}^N (g_{k+i} - g_i) \Delta u(t-i) \\ w'(t) &= \hat{y}(t|t) \end{aligned} \quad (11)$$

Assuming the period of the data loss is D (number of discrete time steps), consequently, the data buffer at the feedback channel preserves the history data, and the accumulated error can be expressed as:

$$\sum_{i=1}^D e(t-i) \quad (12)$$

When the transmission is back to normal, $e(t)$ in Equation 8 can be re-calculated as:

$$e(t) = \beta(y_m(t) - \hat{y}(t|t)) + \beta \sum_{i=1}^D e(t-i)$$

or

$$e(t) = \beta \sum_{i=0}^D [y_m(t-i) - \hat{y}(t-i|t-i)] \quad (13)$$

The compensation has been added in Equation 13. There is no compensation for $e'(t)$ and for the reference trajectory.

4.3 Compensator at the feed-forward channel

The objective of the compensator at the feed-forward channel intends to reduce the effect of the control signals blank caused by the Internet transmission. Equation 6 shows that $\Delta \mathbf{u}$ is a vector composed of the future control increments, whose size is equal to the control horizon. Actually, only the first control increment, however, is taken into action, the rest of them are not in use. Therefore, it is possible to use the rest of the control signals to deal with the transmission data loss and time delay.

Defining the control increments vector as:

$$\Delta \mathbf{u} = [\Delta u(t) \quad \Delta u(t+1) \quad \cdots \quad \Delta u(t+m-2) \quad \Delta u(t+m-1)]^T \quad (14)$$

When the data loss and time delay occur, the previous control vector will be used to control the process by shifting the vector one step forward, which can be written as:

$$\Delta \mathbf{u} = [\Delta u(t+1) \quad \Delta u(t+2) \quad \cdots \quad \Delta u(t+m-1) \quad 0]^T \quad (15)$$

The control increment taken into action will be $u(t+1)$ and the last element of the vector is filled with zero. In the remote side the controller will adopt the latest available signals for its calculation, and keep sending the latest control action to the local side. Once the transmission recovers all the control actions will be received by the local side and those, which are out of date, will be simply omitted.

Ideally, the control action pushes the process to the right direction so that the effect of the control signal blank can be reduced. However, it may lead toward serious problems such as process unstable because of the mismatch between the prediction model and the process and/or the heavy process noise. This problem can be solved through the tuning of the control horizon. In the worse case, the control horizon can be set as one, so that the control signal will be maintained at a fixed value. The control system is degraded into an open control or manual control operation.

5. SIMULATION STUDY

The objectives of the simulation study are to investigate the effect of the Internet time delay and data loss on the control system and to evaluate the performance of the two compensators at the feedback and feed-forward channels. The major benefit of this simulation study includes: (1) isolating the control issues from the Internet communication; (2) amplifying the frequency of the Internet time delay and data loss; (3) providing an identical circumstance for the evaluation. The set-point step change and the step disturbance have been introduced in the simulation in order to assess the control system performance.

5.1 Design of the simulation

The simulation study is conducted in the Matlab/Simulink environment. The system structure is shown in Fig 3, including two compensators, two delay elements, a DMC, and a process model. The process model is stable. The sampling interval T_s is chosen as 1 second, the process variable was collected at the same rate. In order to provide an identical simulation circumstance for various simulation tasks, an identical time delay pattern was employed at both the feedback and feed-forward channels, which was randomly generated. Fig 4(a) illustrates the feedback delay pattern; Fig 4(b) shows the feed-forward delay pattern. In the simulation study, the prediction horizon p is chosen as 10; the control horizon m 5; the reference trajectory

parameter, α , 0.7; the parameter β 1. The set-point step change is 1, and the step disturbance is 0.5.

There are four proposed scenarios: the time delay and data loss do not exist, only exist at the feedback channel, only exist at the feed-forward channel, and exist at both channels. Corresponding to the real world, the first scenario refers the ideal situation, the second one refers Asymmetrical Digital Subscriber Lines (ASDL) communication and the feed-forward channel obtains a high bandwidth; the third one refers ASDL communication and the feedback channel obtains a high bandwidth; the last one refers to the symmetrical communication.

5.2 Simulation Result

Fig 5 shows the simulation results for the scenario, in which the time delay and data loss only exist at the feedback channel. The first disturbance is caused by the set-point step change, the second by the step disturbance. Since the simulation circumstance is identical to various simulation tasks, it is assumed that the differences in the responses are purely

produced by the feedback delay and data loss, and the employment of the compensator. As the result, the feedback compensator can significantly reduce the influence caused by the set-point step change and the step disturbance. The difference between the one with a compensator and the one with no delay is still obvious.

Fig 6 gives the simulation results for the case, in which the time delay and data loss only exist at the feed-forward channel. The time delay and data loss causes the process variable oscillation, which potentially leads the process towards unstable. The effect in the response with the compensator has been dramatically reduced in the set-point step change and the step disturbance. However, the effect has not been fully compensated.

Fig 7 represents the simulation results for the case in which the time delay and data loss exists at both channels. As expected, outputs become worse (more oscillation and overshoot), although they finally reach a stable point. The response with the compensators maintains the performance at an accepted level.

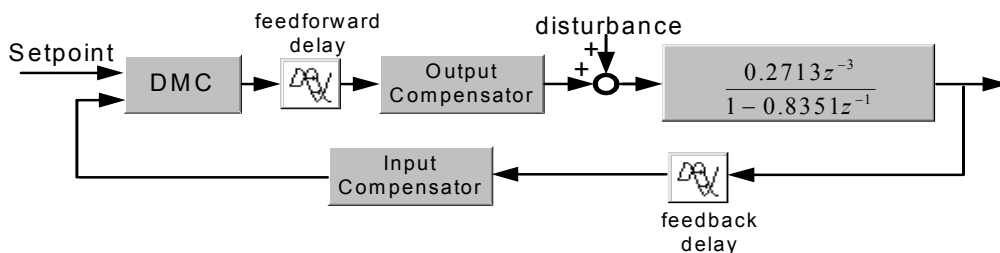


Fig. 3. Simulation structure.

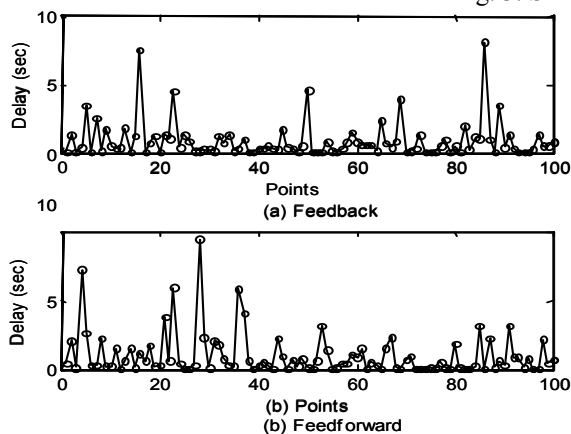


Fig. 4. Input and Output delay pattern.

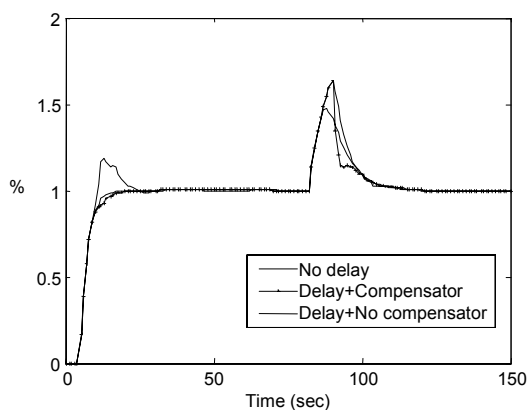


Fig. 5. Comparison of feedback delay effect.

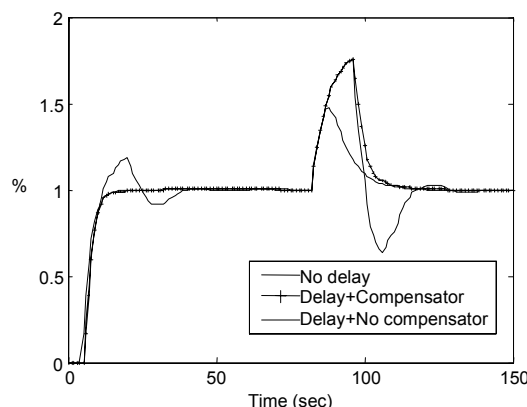


Fig. 6. Comparison of feed-forward delay effect.

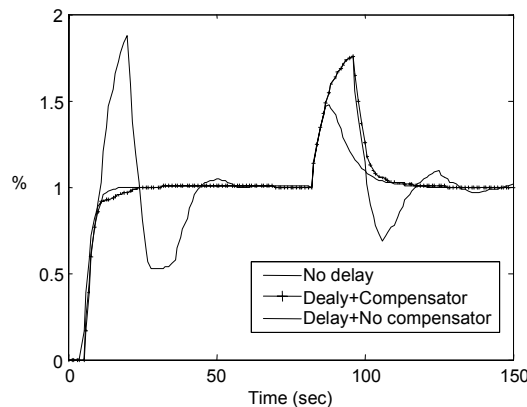


Fig. 7. Comparison of feedback plus feed-forward delay effect.

6. CONCLUSIONS

The conventional discrete control structure is not suitable for Internet-based control systems since it does not consider the Internet transmission features such as uncertain time delay and data loss. In order to handle the Internet transmission features, a novel control structure has been proposed to offer a solution for Internet-based control systems. Taking advantage of the new control architecture, two compensators have been designed to compensate the effect of the Internet time-delay and data loss at the feedback and feed-forward channels. A simulation study has been conducted to evaluate the control architecture and two compensators. The simulation results show that the compensators in the new architecture can significantly reduce the effect of the Internet time-delay and data loss. Another interesting finding is that the feed-forward time delay and data loss seem to cause more serious influence to the control performance, and is more difficult to be compensated in the controller design. Therefore, the feed-forward channel is desired to give a high bandwidth if possible.

NOMENCLATURE

b_i	bandwidth of the i th link
C	speed of light
D	period of data loss
$d_L(k)$	a time-dependent term in the Internet time delay
d_N	a time-independent term in the Internet time delay
$e(t)$	adjustment value of the prediction model
$e'(t)$	adjustment value of the reference trajectory
f	system free response without the time delay and data loss
f'	system free response with the time delay and data loss
f	vector of f
$g_i(i=1, \dots, N)$	process output for a step input
G	system dynamic matrix
I	identity matrix
k	instant
l_i	the i th length of link
m	control horizon
n	number of nodes
N	process horizon
p	prediction horizon
r	set-point
$T_d(k)$	Internet time delay at instant k
$t_i^L(k)$	delay caused by the i th node's load
t_i^R	routing speed of the i th node
T_s	sampling interval
Δt	Tolerant period of sampling time
Δu	increment of input variable
Δu	vector of Δu
w	reference trajectory values
w	vector of reference trajectory

y	output variable
\hat{y}	estimated output variable
y_m	measured output variable
\hat{y}	vector of \hat{y}
α	parameter between 0 to 1
β	parameter between 0 to 1
<i>Superscripts</i>	transposition of matrix
T	

ACKNOWLEDGEMENTS

The contribution is part of the work of the EPSRC (Grant No. GR/R13371/01) funded project "design of Internet-based process control".

REFERENCES

- Acharya, A and Saltz, J., (1996). A Study of Internet Round-trip Delay, *CS-TR-3736*.
- Chen, X., and Yang, S.H., (2002). "Control perspective for virtual process plants", The 5th Asia-pacific Conference on Control and Measurement, China, 256-261.
- Cushing, M. (2000). Process control across the Internet. *Chemical Engineering*, May, 80-82.
- Cutler, C.R. and Ramaker, B.C., (1980). Dynamic Matrix Control – A Computer Control Algorithm. In Automatic Control Conference, San Francisco.
- Halley, A. and P. Gauld, (1999). Integration Where Java Meets Process Control. *Control and Instrumentation*, **31**, 57-58.
- Luo, R. C. and T. M. Chen, (2000). Development of a multi-behaviour-based mobile robot for remote supervisory control through the Internet. *IEEE transactions on mechatronics*, **5**, 376-385.
- Overstreet, J.W., and A. Tzes, (1999). An Internet-based real-time control engineering laboratory. *IEEE Control Systems Magazine*, **19**, 320-326.
- Shaheen, M., K. A. Loparo, and M. R. Buchner, (1998). Remote laboratory experimentation. *American Control Conference, Philadelphia, PA*, 1326-1329.
- Yang, S.H., and J.L. Alty, (2002). Development of a Distributed Simulator for Control Experiments through the Internet. *Future Generation Computer Systems*, **18**, 595-611.
- Yang, S.H., Chen, X., and Alty, J.L., (2003). Design issues and implementation of internet-based process control systems. *Control Engineering Practice*, **11**(6), 709-720.

Model-based Auto-tuning System Using Relay Feedback

Hsioa-Ping Huang, Kuo-Yaun Luo

*Pse, Department of Chemical Engineering, National Taiwan University,
Taipei Taiwan 10617, R.O.C.*

Abstract: An on-line model based autotune system that employs conventional ATV test is proposed. The ATV responses from normalized FOPDT and SOPDT processes are grouped into two zones in a space, which has normalized amplitude and normalized period as coordinates. In terms of the amplitude and the period of constant cycles of an ATV test, model-based tuning rules are also prepared for two types of process, one for FOPDT in one zone and one for under-damped SOPDT in the other zone. Thus, from an ATV test, the amplitude and period of constant cycles are used in an identification step to select tuning rules to be applied to a given process. Then, PID controller settings are computed according to the selected tuning rules. The system can be implemented as simple as the conventional autotune system, and the resulting control performance is compatible to that from a model-based controller design.

Keywords: Relay Feedback, Inverse-based PID Controller, On-line Autotuning

1. INTRODUCTION

The PID auto-tuning has shorten the time to commission control system, and facilitated control optimization through regular retuning. The relay feedback auto-tuning method proposed by Åström and Hägglund was attractive owing to its simplicity and robustness. The important ingredients in the auto-tuning system are identification (parametric or non-parametric) and rules for controller tuning. Many researches on these two aspects have been reported in recent years. For examples, improvements on the accuracy and efficiency by saturation relay feedback test (Yu, et al., 1995) or by reducing high-order harmonic terms or using the Fourier analysis (Lee, et al., 1995; Sung, et al., 1995; Wang, et al., 1997) have been reported. On the other hand, extensive works on the PID tuning formulae and refinement have been published. Extensions of Auto-tuning system to other different cases, such as: time varying delay (Leva, 1993), cascade controllers (Hang, et al., 1994), the Smith Predictor (Plamor, et al., 1994) and the FSA (finite spectrum assignment) controller (Wang, et al., 1995) have also been found in literature. It used to observe that use of model-based tuning rules results in better control performance. But, the trade-off is lots of efforts are required to identify an appropriate model to apply these model-based tuning rules. As has been mentioned, although methods of identification using relay or ATV test has been extensively addressed in literature, the absence of an model-based auto-tuning system as simple and robust as the one of Åström and Hägglund is a simple fact. In this paper, we will reformulate the inverse-based tuning rules in terms of ultimate gain and frequency so that can be easily

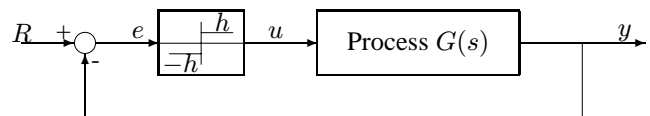


Figure 1: Relay Feedback System

applied using those data obtained from a simple ATV test. On the other hand, a simple method based on the same ultimate gain and frequency obtained is proposed to select the tuning rules which are formulated specifically for different simple dynamics.

2. RELAY FEEDBACK IDENTIFICATION

2.1 Ideal Relay Test

In 1984, Åström and Hägglund (Åström et al., 1984) suggest the relay feedback test to generate sustained oscillation as an alternative to the conventional continuous cycling technique. This relay feedback test was soon (Luyben, 1987) referred as autotune variation (abbr. ATV) test. As shown in Fig.6 is the ATV test. Controller tuning using ATV test is attractive, because it is operated under closed loop and no a priori knowledge of system is need. The test provides ultimate gain and ultimate period for applying Z-N rules to tune a PID controller.

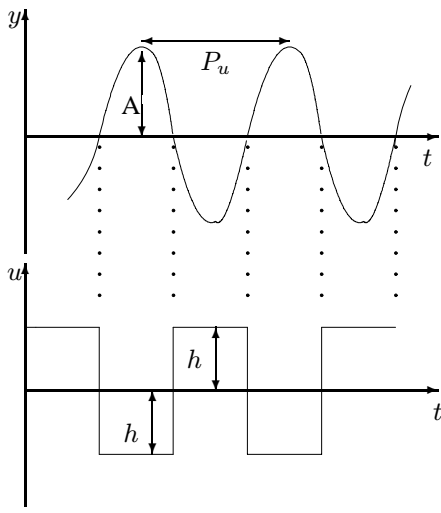


Figure 2: Autotune with ATV Test

The ultimate gain and ultimate frequency are estimated from the ATV test as:

$$k_{cu} = \frac{4h}{\pi A} \quad (1)$$

$$\omega_u = \frac{2\pi}{P_u} \quad (2)$$

By making use of the data obtained, PID controller parameters can be computed using Z-N rules. The control performance thus obtained is in general crude compared with those tuned with model-based rules, such as IMC. This fact is most obvious when the process has underdamped second order dynamics. But, with one simple ATV test, it is usually not sufficient for identifying parametric model of processes other than one that has exactly FOPDT dynamics. This makes spaces for research on developing the parametric models from ATV tests. There are quite a few researchers (e.g. Luyben, 1987; Li, et al., 1991, Ching et al., 1992; Lee and Sung, 1993, Shen et al., 1996, Sung and Lee, 1997, Wang, et al., 1997, Huang, et al., 2000) worked on this problem. Nevertheless, methods from those published works have different extents of sophistication and complexities, and is not convenient for application to autotune systems, where a simple and robust method is desirable. As a result, there remains space for developing effective parametric autotune methods to enhance the controller tuning and achieve better performance.

In model-based methods, tuning formulas are derived for each specific type of transfer function model. But, as far as control performance is concerned, to differentiate FOPDT dynamics from the overdamped dynamics seems not so crucial. In general, the FOPDT-based formula works quite well for over-damped or over-damped-like processes, but not for under-damped ones. Tuning rules for underdamped SOPDT process are indeed required. In this sense, the identification in a autotune system needs only to select models from two types, that is the FOPDT one or an under-damped SOPDT one. In the following, we shall illustrate this identification using one ATV test.

2.2 Relay Feedback Response Curves

Consider the FOPDT and SOPDT models for representing general dynamics in chemical plants. The original and normalized models are shown in the following.

► FOPDT Model

$$G(s) = \frac{K_p e^{-\theta s}}{\tau s + 1}$$

$$G(\bar{s}) = \frac{K_p e^{-\bar{s}}}{\bar{\tau} \bar{s} + 1}$$

$$\text{where } \bar{s} = \theta s, \bar{\tau} = \frac{\tau}{\theta}$$

► SOPDT Model

$$G_p(s) = \frac{K_p e^{-\theta s}}{\tau^2 s^2 + 2\tau\zeta s + 1}$$

$$G_p(\bar{s}) = \frac{K_p e^{-\bar{s}}}{\bar{\tau}^2 \bar{s}^2 + 2\bar{\tau}\zeta \bar{s} + 1}$$

$$\text{where } \bar{s} = \theta s, \bar{\tau} = \frac{\tau}{\theta}.$$

For these two types of processes, extensive ATV tests have been conducted over wide ranges of normalized parameters. For example, for SOPDT process, $\bar{\tau}$ ranges from 0.1 to 100 and ζ from 0.1 to 100. The resulting normalized ultimate gains and ultimate period are plotted and is as shown in Figure(3).

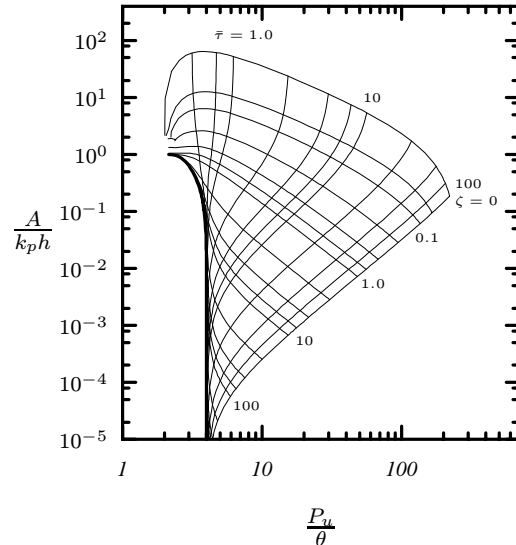


Figure 3: Generalized ATV Responses

2.3 Identification

In Figure(3), it is thus possible to divide the ATV results into different zones. As has been mentioned, for PID controller tuning, overdamped processes and some of underdamped processes that has damping factors close to one can be approximated by FOPDT model. To differentiate the FOPDT and overdamped SOPDT dynamics from those of underdamped SOPDT, the curve having ζ of 0.7 is selected as a criterion. This is because that, in Bode's plot, an SOPDT process does not have resonance peak when its ζ is greater than or equal 0.707. Thus, as shown in Figure (4), there are two zones (Zone I and Zone II) separated by two curves. Among the curves, one is on the edge of zone I that represents FOPDT dynamics. The normalized time constant (i.e. $\bar{\tau}$) of this FOPDT process ranges from 0.1 to 100. The other is on the edges of the zoneI and Zone II. Zone II represents processes of underdamped dynamics. With Figure (4), identifying an unknown system using ATV test can thus be conducted using the resulting A and P_u . By locating the experimental results on the figure, parameters can be estimated, provide that k_p and θ is known, using the following equations. In case of both values of k_p and θ are not available, estimation method will be introduced later in the section of tuning procedures.

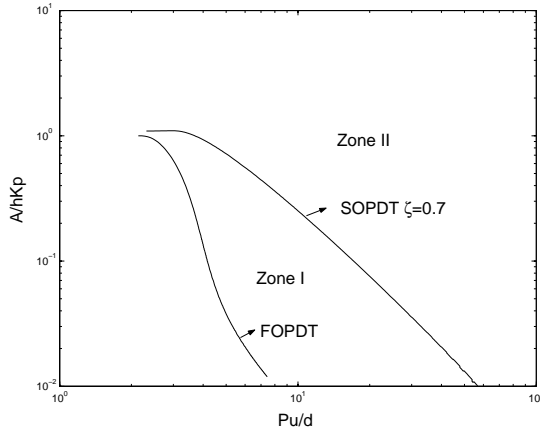


Figure 4: Simplified ATV Responses

1. For point located in FOPDT zone:

$$\tau = \frac{\sqrt{K_u^2 - 1}}{\omega_u} = \frac{P_u}{2\pi} \sqrt{K_u^2 - 1}$$

$$\theta = \frac{\pi - \tan^{-1} \sqrt{K_u^2 - 1}}{\omega_u}$$

where, $K_u = k_p k_{cu}$

2. For point located in underdamped SOPDT zone:

$$2\tau\zeta\omega_u = Y = K_u \sqrt{\frac{\tan^2(\gamma)}{1 + \tan^2(\gamma)}}$$

$$\tau\omega_u = X = \sqrt{1 + \frac{Y}{\tan(\gamma)}}$$

where, $K_u = k_p k_{cu}$ and $\gamma = \omega_u \theta$

3. TUNING RULES

An inverse-based design is used to synthesize PID controller for autotune. The controller is synthesized so as to have a loop transfer function (abbr. LTF) of two standard forms of the following. That is:

$$G_{loop}(s) = \frac{0.65 (1 + 0.4\theta s e^{-\theta s})}{\theta s(1 + \tau_f s)} \quad (3)$$

or,

$$G_{loop}(s) = \frac{0.4 e^{-\theta s}}{\theta s(1 + \tau_f s)} \quad (4)$$

These loop transfer function can provide the system reasonable stability robustness and control performance. According to these standard forms, the PID controller is synthesized for FOPDT dynamic process and is given as follows:

$$G_c(s) = K'_c \left(1 + \frac{1}{\tau'_R s} + \frac{\tau'_D s}{1 + \tau_f s}\right) \quad (5)$$

where,

$$(K'_c) = 0.65 * \frac{\theta}{\tau} * \frac{1}{K_p}$$

$$(\tau'_R) = \tau$$

$$(\tau'_D) = 0.4\theta$$

On the other hand, the PID controller for SOPDT type dynamic process is:

$$G_c(s) = K_c \left(1 + \frac{1}{\tau_R s} + \tau_D s\right) (1 + \tau_f s) \quad (6)$$

$$K_c = \frac{2\tau\zeta}{K_p\theta} * 0.4$$

$$\tau_R = 2\tau\zeta$$

$$\tau_D = \frac{\tau^2}{2\tau\zeta}$$

Since, all controller parameters are in terms of the dynamic parameters as identified in the previous section, these controller parameters can be re-formulated to be in terms of ultimate gain and ultimate period. In other words, the tuning parameters can be directly computed from the results of a ATV test. As an example, for FOPDT process, the PID parameters can be re-written as:

$$K'_c = (K_c)_{ZN} \times 0.54$$

$$\tau'_R = (\tau_R)_{ZN} \times F_1$$

$$\tau'_D = (\tau_D)_{ZN} \times F_2 \quad (7)$$

where,

$$F_1 = \frac{\sqrt{K_{cu}^2 K_p^2 - 1}}{\pi}$$

$$F_2 = \frac{1.6}{\pi} \left[1 - \frac{\tan^{-1} \sqrt{K_{cu}^2 K_p^2 - 1}}{\pi} \right]$$

A comparison of this inverse-based tuning with that of Z-N tuning is as shown in Figure(5).

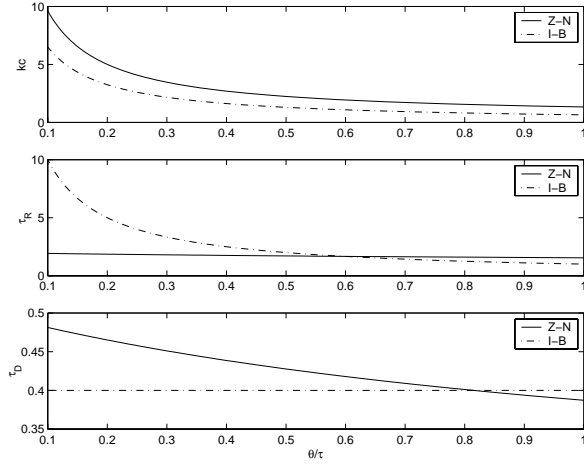


Figure 5: Comparisons of Inverse-based And Z-N Controller Settings

4. AUTOTUNE PROCEDURES

As has been mentioned, when the values of k_p and the apparent deadtime, θ , are available, the autotune procedure proceeds just like the conventional one, except that the selection of tuning rules by locating $(A/(k_p h), P_u/\theta)$ on Figure (4) is required as a preceding step, and the tuning rules itself are different.

In case of where k_p and θ are not available, the ATV test has to make a slightly modification. The excitation to the relay feedback system is introduced through an external input at the output of relay. As shown in Figure (6). The external input has to be small like up to 10% of h , the level of relay output. Nomenclatures for computing amplitudes and period are given in Figure (??). Then, k_p is estimated by the following equation:

$$k_p = \frac{\int_t^{t+P/2} y(\tau) d\tau}{\int_t^{t+P/2} u(\tau) d\tau} \quad (8)$$

On the other hand, the apparent deadtime for applying the identification zones in Figure (4) are estimated as an average value of true deadtime detected at the very beginning of the test and q quarter of period later at constant cycling, as shown in Figure.(??). This is because the deadtime interms of SOPDT dynamics is always lying between the two values aforementioned.

To calculate the amplitudes for identification, the centerline of the cycling has to be updated to to the bias form the input to a height of $y_\delta = 0.5(A_1 - |A_2|)$.

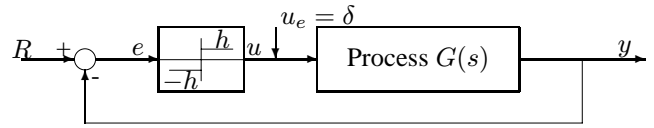


Figure 6: ATV Test with External Excitation

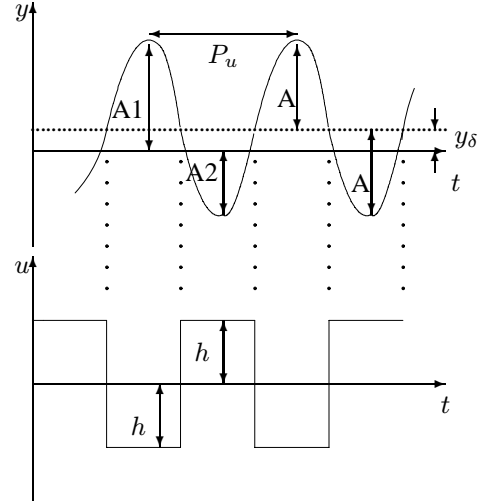


Fig 7: External Excitation ATV Test

Besides the preceding steps just mentioned, all other remaining procedures are the same as the previously described ones. Thus, by estimating the normalized amplitude and the normalized period, and by making use of Figure (4), tuning rules can be selected and controller parameters can be computed.

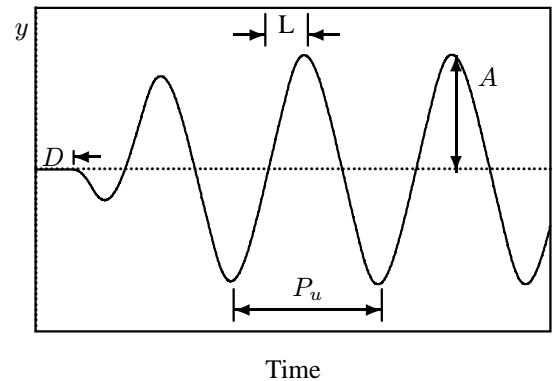


Fig 8: Estimation for Apparent Deadtime

5. SIMULATION RESULTS

The following are the results of applying this autotune procedure to a few example processes.

Ex.1

$$\text{Process } \frac{1}{(s+1)^5} e^{-s}$$

Table1: Simulation Results

K_p	a	h	K_{cu}	K_u	ω_u
1.0000	0.6444	1.000	1.9758	1.9758	0.5689

P_u	L	D	d
11.0444	2.8337	1.500	2.0206

Table2: PID Parameters and IAE values

	Z-N	proposed
k_c	1.1623	0.3348
τ_I	5.5222	2.2904
τ_D	1.3805	1.4776
IAE	8.518	6.685

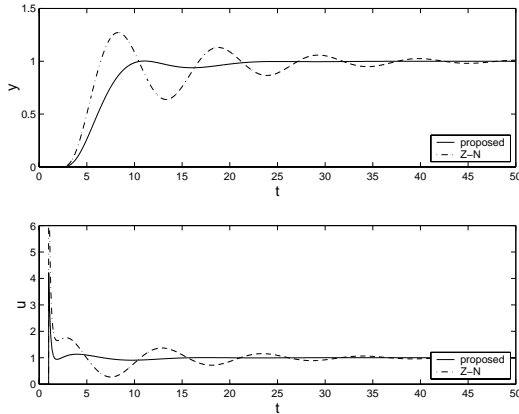


Figure 7: Ex.1 Tuning result

Ex.2

$$\text{Process } \frac{1.08}{(s+1)^2(2s+1)^3} e^{-10s}$$

Table3: Simulation Results

K_p	a	h	K_{cu}	K_u	ω_u
1.0826	1.0487	1.000	1.2141	1.3144	0.1807

P_u	L	D	d
34.78	11.2275	11	11.1138

Table 4: PID parameters and IAE values

	Z-N	proposed
k_c	0.7141	0.2094
τ_I	17.3900	4.6926
τ_D	4.3475	5.3974
IAE	38.325	21.749

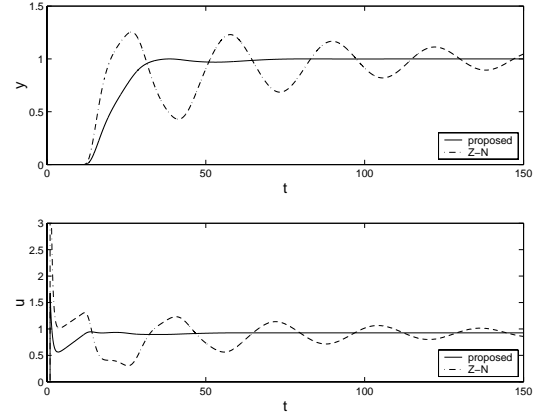


Figure 8: Ex.2 Tuning result

Ex.3

$$\text{Process } \frac{1}{(s^2 + 0.6s + 1)} e^{-s}$$

Table5: Simulation Results

K_p	a	h	K_{cu}	K_u	ω_u
1.0000	1.727	1.000	0.7373	0.7373	1.1464

P_u	L	D	d
5.4806	1.3609	1.000	1.1805

Table6: PID parameters and IAE values

	Z-N	proposed
k_c	0.4337	0.2128
τ_I	2.7403	0.6280
τ_D	0.6851	1.4044
IAE	7.3250	4.0262

5. CONCLUSION

In this paper, we have presented a autotune system which make uses of model-based tuning rules to enhance control performance. The presented system works in a similiar way to the one of Astrom and Hugglund in the sense it uses a conventional AYV test and the resulting amplitude and period of constant cycles. Because of using parametric models, additional steps it needs are the estimation of k_p and θ . The tuning rules are derived from an inverse-based approach,

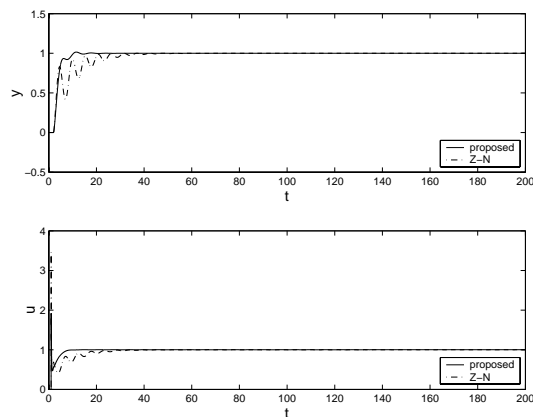


Figure 9: Ex.3 Tuning result

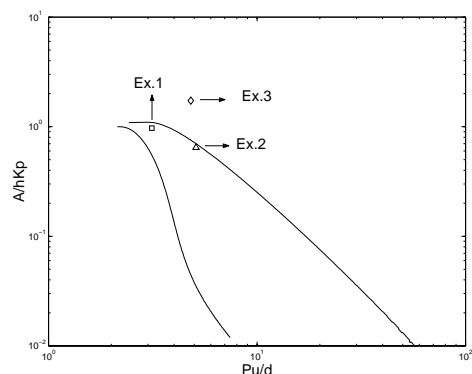


Figure 10: Identification Results

which is similar to the IMC method but simpler. From the simulation results, we can observe and conclude that this autotune system is efficient and self-contained.

6. REFERENCE

Åström and K.J., T. Hägglund (1984), Automatic tuning of simple regulators with specifications on phase and amplitude margins, *Automatica*, **20**,645-651

Ching, R.C., S.H. Shen and C.C. Yu (1992), Derivation of transfer function from relay feedback systems, *Ind. Eng. Chem. Res.*, **31**,855-860

Huang C.C., A.P. Loh and V.U. Vasnani (1994), Relay feedback auto-tuning of cascade controllers, *IEEE Trans. Control System Tech.*, **2**,42-45

Huang, H.P., M.W. Lee and I.L. Chien (2000), Identification of transfer function models from the relay feedback test, *Chem. Eng. Comm.*, **180**,231-253

Huang, H.P., M.W. Lee and Y.T. Tang (2000), Identification of Wiener model using relay feedback test, *J. of Ch. E. Japan*, **31**,604-612

Lee, J., S.W. Sung (1993), Comparison of two identification methods for pid controller tuning, *AIChE J.*, **39**,695-697

Lee, T.H., Q.G. Wang and K.K. Tan (1995), A modified relay-based technique for improved critical point in process control, *IEEE Trans. Control System Tech.*, **3**,330-337

Leva, A. (1993), PID auto-tuning algorithm based on relay feedback, *IEE Proc. Pt. D.*, **140**,328-338

Li, W., E. Eskinat and W.L. Luyben (1991), An improved autotune identification method, *Ind. Eng. Chem. Res.*, **20**,1023-1042

Luyben, W.L. (1987), Derivation of transfer functions for highly nonlinear distillation columns, *Ind. Eng. Chem. Res.*, **26**,2490-2495

Plamor, Z.J. and M. Blau (1994), An auto-tuner for Smith dead time compensator, *Int. J. Control*, **60**,117-135

Schei, T.S. (1992), A method for closed loop automatic tuning of PID controllers, *Automatica*, **28**,587-591

Shen, S.H., J.S. Wu and C.C. Yu (1996), Use of biased relay feedback for system identification, *AIChE J.*, **42**,1174-1180

Shen, S.H., H.D. Yu and C.C. Yu (1996), Use of saturation-relay feedback method for autotune identification, *Chem. Eng. Sci.* **51**,1187-1198

Shen, S.H., J.S. Wu and C.C. Yu (1996), Autotune identification under load disturbance, *Ind. Eng. Chem. Res.*, **35**,1642-1651

Sung, S.W. and I.B. Lee (1997), Enhance relay feedback method, *Ind. Eng. Chem. Res.*, **36**,375-381

Sung, S.W., J.H. Park and I. Lee (1995), Modified relay feedback method, *Ind. Eng. Chem. Res.*, **34**,4133-4135

Wang, Q.G., C.C. Huang and B. Zou (1997), Low-order modeling from relay feedback, *Industrial and Engineering Chemistry Research*, **36**,375-381

Wang, Q.G., C.C. Huang and B. Zou (1997), A frequency response approach to auto-tuning of multivariable controllers, *Chemical Engineering Research and Design*, **75**,797-806

Wang, Q.G., T.H. Lee and K.K. Tan (1995), Automatic tuning of finite spectrum assignment controllers for delay system, *Automatica*, **28**,477-482

Wang, Q.G. and Y. Zhang (2001), Robust identification of continuous systems with deadtime from step responses, *Automatica*, **37**,377-390

THE EXPLICIT MODEL-BASED TRACKING CONTROL LAW VIA PARAMETRIC PROGRAMMING

Vassilis Sakizlis John D. Perkins
Efstratios N. Pistikopoulos¹

*Centre for Process Systems Engineering,
Department of Chemical Engineering, Imperial College London,
South Kensington campus, London SW7 2AZ, U.K.*

Abstract: In this paper two methods are presented for deriving the explicit model-based tracking optimal control law for constrained linear dynamic systems subject to persistent disturbances. The first scheme augments explicitly the model dynamics with a set of integral states that are then readily incorporated with a positive definite penalty in the system performance measure. The second scheme employs a state observer for estimating the value of the disturbance and then computes the new state target. Then it shifts accordingly the state and control values to ensure asymptotic tracking. The underlying controller structure in both approaches is derived off-line via parametric programming before any actual process implementation takes place. The proposed control schemes guarantee steady-state offset elimination and optimal performance in the presence of unknown constant uncertainties.

Keywords: Model predictive control, parametric programming, process control, integral action, observer.

1. INTRODUCTION

Contrary to conventional control design methods, model predictive control (MPC) (Lee and Cooley, 1997) is particularly effective for dealing with a broad class of complex multivariable constrained processes. MPC determines the optimal future control profile according to a prediction of the system behaviour over a receding time horizon. The control actions are computed by solving repetitively an on-line optimal control problem over a receding horizon every time a state measurement or estimate becomes available. The capabilities of MPC are limited mainly by the significant on-line calculations that make it applicable mostly to slowly varying processes. This

shortcoming is surpassed by employing a different type of model-based controllers the so-called parametric controllers (see section 2) (Pistikopoulos *et al.*, 2002; Bemporad *et al.*, 2002b). These controllers are based on recently proposed novel parametric programming algorithms, developed in our research group at Imperial College, and succeed in obtaining the explicit mapping of the optimal control actions in the space of the current states. Thus, a state feedback control law for the system is derived off-line, hence avoiding the restrictive on-line computations.

However, the inevitable presence of persistent unmeasured disturbances, pertaining for instance to model inaccuracies, parameter drift, input variations, have largely been ignored while designing the parametric controllers. Consequently, the performance of this novel control technique may lead to infeasibilities and permanent offset from

¹ To whom correspondence should be addressed. Tel.: (44) (0) 20 7594 6620, Fax: (44) (0) 20 7594 6606, E-mail: e.pistikopoulos@ic.ac.uk

the target due to inaccurate forecasting of the process behaviour. The infeasibilities may result in situations such as off-spec production or hazardous plant operation. Hence, a modification of the explicit control law is necessary to ensure feasible and safe operation.

In this work novel methodologies are presented for designing tracking model based parametric controllers for general linear dynamic systems. The control policy is derived off-line as a function of the process states via our parametric programming based theory and techniques (Dua et al., 2002; Sakizlis et al., 2002a). The proposed control scheme achieves satisfactory disturbance attenuation, while eliminating any steady state offset from the target. This is achieved via two methods: (i) As described in section 3 the first method incorporates explicitly integral action in the control design formulation while (ii) the alternative approach presented in section 4 uses an observer for estimating the disturbance vector and a reference target computation for removing the offset. A comparison of the two schemes is performed in section 5 while a demonstrative example (section 6) is presented and some conclusions (section 7) are drawn in the next paragraphs.

2. PRELIMINARIES

For deriving the explicit model - based control law for a process system, the following receding horizon optimal control problem is formulated (Bemporad *et al.*, 2002):

$$\begin{aligned}
\hat{\phi}(x_{t|t}) &= \min_{v^N \in V^N} x_{t+N|t}^T P x_{t+N|t} \\
&\quad + \sum_{k=0}^{N-1} [y_{t+k|t}^T Q y_{t+k|t} + v_{t+k}^T R v_{t+k}] \\
\text{s.t.} \\
x_{t+k+1|t} &= A_1 x_{t+k|t} + A_2 v_{t+k} \\
y_{t+k|t} &= B_1 x_{t+k|t} + B_2 v_{t+k} \\
0 &\geq g(y_{t+k|t}, x_{t+k|t}, v_{t+k}) = \\
&\quad C_0 y_{t+k|t} + C_1 x_{t+k|t} + C_2 v_{t+k} + C_3 \\
&\quad k = 0, 1, 2, \dots, N-1 \\
0 &\geq \psi^e(x_{t+N|t}) = D_1 x_{t+N|t} + D_2 \\
x_{t|t} &= x^*; \tag{1}
\end{aligned}$$

where $x \in \mathbb{R}^n$ are the states, $y \in \mathbb{R}^m$, are the outputs and $v \in V \subseteq \mathbb{R}^q$ are the controls; t is the time when a measurement is taken, k is the future time instants and N is the prediction horizon. The outputs are the variables that we aim to control, i.e. to drive to their set-point, (temperatures, concentrations) whereas the states are the variables that fully characterize the current process conditions (enthalpies, specific volume).

$v^N = [v_{t+k}^T, v_{t+k+1}^T, \dots, v_{t+k+N-1}^T]^T$ denotes the sequence of the control vector over the receding horizon. The constraints $g : \mathbb{R}^m \times \mathbb{R}^n \times V \mapsto \mathbb{R}^r$, $\psi^e : \mathbb{R}^n \times V \mapsto \mathbb{R}^{Q_e}$, which may pertain to product specifications or actuator restrictions, and bounds on v define the feasible operating region. We assume that the pair (A_1, A_2) is stabilizable and the pair (A_1, B_1) detectable. By considering the current states x^* as parameters and eliminating the equalities in (1) by substituting $x_{t+k|t} = A_1^k x^* + \sum_{j=0}^{k-1} (A_1^j A_2 v_{t+k-1-j})$ for the states, problem (1) is recast as a multiparametric quadratic program (mp-QP). The solution of that problem (Dua *et al.*, 2002) consists of a set of affine control functions in terms of the states and a set of regions where these functions are valid. This mapping of the manipulating inputs in the state space constitutes a control law for the system. The mathematical form of the parametric controller is as follows:

$$\begin{aligned}
v_t(x^*) &= \mathcal{A}_c x^* + b_c; \text{ if } CR_c^1 x^* + cr_c^2 \leq 0 \\
&\text{for } c = 1, \dots, N_c; \tag{2}
\end{aligned}$$

where N_c is the number of regions in the state space, \mathcal{A}_c, CR_c^1 and b_c, cr_c^2 are constant matrices and vectors respectively and the index c designates that each region admits a different control law. The vector $v_{t|0|c}$ is the first element of the control sequence, whereas similar expressions are derived for the rest of the control elements.

The model-based parametric controller described here fails to address the impact of persistent, unmeasured disturbances on the process dynamic behaviour. These uncertainties (i) tend to cause a permanent deviation of the steady state output values from their target point and (ii) may also cause violation of constraints if the reference signal is close to the feasible region boundaries. For surpassing those shortcomings Bemporad *et al.* (2002b) treated the disturbance as an extra parameter, thus resulting in a control law that has an extra feedforward term in (2). This technique is valid provided the disturbance modelling is perfect and an accurate measurement of the uncertainty is available. Otherwise, it fails to address the issues stressed above. Other techniques are based on anti-windup (Bemporad *et al.*, 2002a), avoiding the incorporation of reference tracking capabilities in the controller structure. In the next sections it is shown how to avert the impact of disturbances by modifying the nominal design of the model based parametric controller.

3. TRACKING PARAMETRIC CONTROLLER WITH INTEGRAL PENALTY

In conventional feedback control schemes, (Seborg *et al.*, 1989) integral action is incorporated for attenuating any permanent deviation of the output variables from their set-points (e.g. PI-controller). Here, the incorporation of the integral action for the same purpose is achieved by introducing an integral state in the plant dynamics that is equal to the accumulated deviations of the output from its reference point, usually the origin. This state is augmented as an additional penalty on the objective function. The open-loop control design optimization problem (1) over the nominal uncertainty scenario, after the incorporation of the integral state is modified as follows:

$$\begin{aligned}
\phi(x^*, \mathbf{xq}^*) &= \min_{v_{t+k}} x_{t+N|t}^T P x_{t+N|t} + \mathbf{xq}_{t+N}^T \mathbf{P}_1 \mathbf{xq}_{t+N} \\
&+ \sum_{k=0}^{N-1} [y_{t+k|t}^T Q y_{t+k|t} + v_{t+k}^T R v_{t+k} \\
&\quad + \mathbf{xq}_{t+k}^T \mathbf{Q}_1 \mathbf{xq}_{t+k}] \\
&\text{s.t.} \\
x_{t+k+1|t} &= A_1 x_{t+k|t} + A_2 v_{t+k} + W \theta_{t+k}^n \\
y_{t+k|t} &= B_1 x_{t+k|t} + B_2 v_{t+k} + F \theta_{t+k}^n \\
\mathbf{xq}_{t+k+1} &= \mathbf{xq}_{t+k} + \mathbf{y}_{t+k|t} \\
x_{t|t} &= x^*, \quad \mathbf{xq}_{t|t} = \mathbf{xq}^* \\
0 &\geq g(y_{t+k|t}, x_{t+k|t}, v_{t+k}); \quad 0 \geq \psi^e(x_{t+N|t}) \\
k &= 0, 1, 2, \dots, N-1 \\
\mathbf{xq}_{t+k} &\in \mathbf{Re}^m
\end{aligned} \tag{3}$$

where xq is the integral state; Q_1, P_1 are the quadratic costs corresponding to that state. By treating the *pure* and the *integral* states as parameters, problem (3) is recast as a multiparametric quadratic program. The solution of that problem derives a set of piecewise affine control functions in terms of the states and a set of critical regions where these expressions hold. These functions constitute a state feedback controller whose mathematical form is as follows:

$$\begin{aligned}
v_t(x^*, xq^*) &= \mathcal{A}_c \cdot x^* + b_c + \mathcal{D}_c \cdot \mathbf{xq}^*; \\
\mathcal{CR}_c &\equiv \{CR_c^1 \cdot x^* + cr_c^2 + \mathbf{CR}_c^3 \cdot \mathbf{xq}^* \leq 0 \quad (4) \\
&\quad \text{for } c = 1, \dots, N_c\}
\end{aligned}$$

The piecewise affine multivariable controller represented by (4) contains a proportional part $\mathcal{A}_c \cdot x^*$ with respect to the states, an output integral part $\mathcal{D}_c xq^*$ and a bias b_c . The presence of the integral term guarantees off-set free tracking of the output set point giving rise to a tracking parametric controller. Note that the control law is partitioned to a set of regions that are completely

defined by a set of constant matrices and vectors $[x^* \quad xq^*]^T \in \mathcal{CR}_c, \mathcal{CR}_c \equiv \{CR_c^1, cr_c^2, CR_c^3\}$.

Theorem 3.1. The control law defined by (4) is asymptotically stable, thus it guarantees no steady state offset from the target point in the presence of constant disturbances $\theta_t \in \Theta \subset \mathbb{R}^w$, where $\Theta \equiv \theta^L \leq \theta_t \leq \theta^U$ on condition that (i) the dimension of the controls is larger or equal to the output dimension $q \geq m$ (ii) the open-loop transfer matrix defined from the equation: $H(z) = B_1(zI - A_1)^{-1}A_2 + B_2$ poses no zeros at the origin, (iii) the quadratic cost matrix Q_1 that penalizes the integral error is positive-definite (iv) the terminal cost and the time horizon length are appropriately tuned according to the criteria in Rawlings and Muske (1993) and Chmielewski and Manousiouthakis (1996) respectively and (v) the reference point of attraction is an interior point of the feasible region space defined as:

$$\begin{aligned}
\hat{y} &\in Y, Y = \{y \in \mathbb{R}^m \cup [y_{t+k|t} = B_1 x_{t+k|t} + B_2 v_{t+k} \quad (5) \\
x_{t+k+1|t} &= A_1 x_{t+k|t} + A_2 v_{t+k} + W \theta_t, g(x_{t+k|t}, v_{t+k}) \leq 0, \\
\psi^e(x_{t+N|t}) &\leq 0, v_{t+k} \in V, \theta_t \in \Theta, k = 1, \dots, N-1\}
\end{aligned}$$

If the target point does not belong to the feasible region $y_{ref} = 0 \notin Y$ then the equilibrium point $\hat{y} \neq 0$ in terms of the control driven outputs will lie on the boundaries of the feasible region. Then Theorem 3.1 still holds provided that for the evaluation of the integral states, the error of the outputs is shifted according to the modified equilibrium point, i.e. $xq_{t+k+1|t} = xq_{t+k|t} + \underbrace{(y_{t+k|t} - \hat{y})}_{\text{error}}$.

4. TRACKING PARAMETRIC CONTROLLER WITH DISTURBANCE ESTIMATOR

The design of an offset free parametric controller integrated with a disturbance estimator is based on the work of Muske and Rawlings (1993) that has been extended recently by the work of Muske and Badgwell (2002) where different types of integrators were added into the plant representations. The steps of our method are:

1. Generate an input or output disturbance model. For that purpose a distinction is made between two systems (i) one being the real process plant and (ii) the other comprising a model that represents an estimate of the process behavior, as shown in Table 1: where vector w is the actual disturbance vector that enters the system, whereas θ is the disturbance estimate. Vector θ is modelled as a step disturbance, thus being constant over

Table 1. Real vs. Prediction Model

Real System	
$\hat{x}_{t+1} = \hat{A}_1 \hat{x}_t + \hat{A}_2 v_t + \hat{W}_1 w_t$	
$\hat{y}_t = \hat{B}_1 \hat{x}_t + \hat{B}_2 v_t + \hat{W}_2 w_t$	
Prediction model	
$x_{t+1} = A_1 x_t + A_2 v_t + W_1 \theta_t$	
$y_t = B_1 x_t + B_2 v_t + W_2 \theta_t$	

the receding horizon, but admitting a different realization every time a piece of information about the process plant is available.

2. Estimate the disturbance. Two different estimation schemes are used here:

- *Least squares recursive estimator.*

$$\begin{aligned} \zeta_{t+1} &= \zeta_t + (\hat{y}_t - y_t) \\ \theta_t &= (B_1 \cdot W_1 + W_2)^P \cdot \zeta_t \end{aligned} \quad (6)$$

where $(B_1 \cdot W_1 + W_2)^P$ is the pseudo-inverse of matrix $B_1 \cdot W_1 + W_2$. This algebraic manipulation performs disturbance estimation via the least squares method (Stengel, 1994).

- *Augmented Kalman Filter Estimator* This scheme provides an estimation for the current states and the disturbances if they are not measured directly. Consider the augmented with the disturbance state space system.

$$\underbrace{\begin{bmatrix} x_{t+1} \\ \theta_{t+1} \end{bmatrix}}_{x_{e,t+1}} = \underbrace{\begin{bmatrix} A_1 & W_1 \\ 0 & I \end{bmatrix}}_{\bar{A}_1} \cdot \underbrace{\begin{bmatrix} x_t \\ \theta_t \end{bmatrix}}_{x_{e,t}} + \underbrace{\begin{bmatrix} A_2 \\ 0 \end{bmatrix}}_{\bar{A}_2} \cdot v_t$$

$$\bar{B}_1 = [B_1 \ W_2] \quad (7)$$

The estimator equations are:

$$\begin{aligned} x_{e,t+1} &= \bar{A}_1(I - \bar{M}\bar{B}_1)x_{e,t} + (\bar{A}_2 - \bar{A}_1\bar{M}\bar{B}_2)v_t \\ &\quad + \bar{A}_1\bar{M}\hat{y}_t \\ \bar{y}_t &= \bar{B}_1(I - \bar{M}\bar{B}_1)x_{e,t} + \bar{B}_1\bar{M}\hat{y}_t \end{aligned} \quad (8)$$

The input to that filter are the measurements from the plant, the inputs to the plant and the previous state/ disturbance estimate: $[\hat{y}_t, v_t, x_{e,t}]$. The output from the filter are the output filtered estimate, the state estimate and the disturbance estimate: $\bar{y} = [x_e, y_e]^T$. \bar{M} is the filter gain that is a function of (i) Q^e, R^e cost matrices of the estimator, (ii) the structure of the input noise to the system.

3. Based on the disturbance value a new steady state point $[x_s \ v_s]$ is computed. If the dimension of the output variables y is equal to the dimension of input controls v and no input and state constraints are violated in the new steady state, then this is done as follows:

$$\begin{bmatrix} I - A_1 & -A_2 \\ B_1 & B_2 \end{bmatrix} \cdot \begin{bmatrix} x_s \\ v_s \end{bmatrix} = \begin{bmatrix} W_1 \cdot \theta_t \\ -W_2 \cdot \theta_t \end{bmatrix} \quad (9)$$

Otherwise if $q = \dim v \geq m = \dim y$ the evaluation of x_s, v_s is done via (Muske and Rawlings, 1993):

$$\begin{aligned} &\min_{x_s, v_s} (v_s - v^o)^T R_s (v_s - v^o) \\ \text{s.t.} &\begin{bmatrix} I - A_1 & -A_2 \\ B_1 & B_2 \end{bmatrix} \cdot \begin{bmatrix} x_s \\ v_s \end{bmatrix} = \begin{bmatrix} W_1 \cdot \theta_t \\ -W_2 \cdot \theta_t \end{bmatrix} \\ &0 \geq g(y^o, x_s, v_s), \quad 0 \geq \psi^e(x_s, v_s) \end{aligned} \quad (10)$$

In the case where there are more measurements than control inputs the evaluation of x_s, v_s is performed via solving:

$$\begin{aligned} &\min_{x_s, v_s} (y^o - B_1 x_s - B_2 v_s - W_2 \theta_t)^T Q_s \\ &(y^o - B_1 x_s - B_2 v_s - W_2 \theta_t) \\ \text{s.t.} &\begin{bmatrix} I - A_1 & -A_2 \end{bmatrix} \cdot \begin{bmatrix} x_s \\ v_s \end{bmatrix} = [W \cdot \theta_t] \\ &0 \geq g(y^o, x_s, v_s), \quad 0 \geq \psi^e(x_s, v_s) \end{aligned} \quad (11)$$

where v^o are the prior-to-disturbance control nominal values, usually taken as $v^o = 0$; y^o are the output nominal set-points, usually $y^o = 0$. Note that problems (9) - (11) are constrained quadratic problems that can be recast as multiparametric quadratic programs (mp-QPs) by treating θ_t as parameters. The analytical solution (Dua et al., 2002) of these problems:

$$\begin{aligned} v_s &= \alpha_v^c \theta_t + \beta_v^c, \quad x_s = \alpha_x^c \theta_t + \beta_x^c \\ \text{if } &\tilde{C}R_c(\theta_t) \leq 0, \quad c = 1, \dots, \tilde{N}_c \end{aligned} \quad (12)$$

4. The state and input constraints are shifted according to the new target point resulting in the following open-loop optimal control formulation (Rawlings, 2000):

$$\begin{aligned} \phi(\bar{x}_{t|t}) &= \min_{\bar{v}_{t|N}} \bar{x}_{t|N}^T P \bar{x}_{t|N} \\ &\quad + \sum_{k=0}^{N-1} [y_{t+k|t}^T Q y_{t+k|t} + \bar{v}_{t+k}^T R \bar{v}_{t+k}] \\ \text{s.t.} & \\ \bar{x}_{t+k+1|t} &= A_1 \bar{x}_{t+k|t} + A_2 \bar{v}_{t+k} \\ y_{t+k|t} &= B_1 \bar{x}_{t+k|t} + B_2 \bar{v}_{t+k} \\ 0 &\geq g[y_{t+k|t}, (\bar{x}_{t+k|t} + x_s), (\bar{v}_{t+k} + v_s)] \\ &= C_0 y_{t+k|t} + C_1 \cdot (\bar{x}_{t+k|t} + x_s) \\ &\quad + C_2 \cdot (\bar{v}_{t+k} + v_s) + C_3 \\ 0 &\geq \psi^e(\bar{x}_{t+N|t} + x_s) \\ &= D_1 \cdot (\bar{x}_{t+N|t} + x_s) + D_2 \\ v_s &= \alpha_v^c \theta_t + \beta_v^c \\ x_s &= \alpha_x^c \theta_t + \beta_x^c \\ \text{if } &\tilde{C}R_c(\theta_t) \leq 0, \quad c = 1, \dots, \tilde{N}_c \\ \bar{x}_{t|t} &= \bar{x}^*; \quad k = 0, 1, 2, \dots, N \end{aligned} \quad (13)$$

Note that the dynamic system is shifted ($\bar{x} = x - x_s, \bar{v} = v - v_s$) to bring the system to the output target point, however, the constraints remain unaltered. As such, (13) can be viewed as a set of \tilde{N}_c quadratic programs each one pertaining to every individual region of (12). Hence, once θ_t

and \bar{x}^* are treated as a parameters, each one of the N_c programs (13) is recast as an mp-QP. The solution of these problems can be unified resulting the following control law:

$$\begin{aligned} \bar{v}_t(\bar{x}^*, \theta_t) = \{ \{ \mathcal{A}_{c,j} \bar{x}^* + \mathcal{B}_{c,j} \theta_t + b_{c,j} \\ \text{if } CR_{c,j}^1 \bar{x}^* + CR_{c,j}^2 \theta_t + cr_{c,j}^3 \leq 0 \\ \text{for } c = 1, \dots, N_c \} \text{ if; } \tilde{C}R(\theta_t) \leq 0, j = 1, \dots, \tilde{N}_j \} \end{aligned} \quad (14)$$

5. REMARKS

- Note in controller (4) that the input and state constraints do not include any integral states. Hence, if the current states lie in a critical region where at least one of those constraints is active the corresponding control functions in (4) do not include any integral term. Thus, when constraint saturation occurs the integral action is switched off automatically by our controller. Hence, our compensator features explicit *anti-reset windup* properties as they are defined in the scheme of Kothare *et al.* (1994).
- In controller (14) note that both estimators incorporate an integrator: ζ in the least squares, θ in the Kalman filter estimator. The compensator can be viewed as the proportional part of the controller and the estimator as the integral part (Vogel and Downs, 2002).
- The main advantage of the tracking parametric controller (4) vs. (14) is that it does not necessitate the existence of a disturbance or uncertainty estimator.
- The tracking parametric controller (4) is easier to tune since its tunings can readily be obtained via a modified Ziegler Nichols or IMC approach.
- The tracking parametric controller with estimator (14) can provide improved performance and feasibility provided the estimator represents exactly the plant and the disturbance profile. In fact in the unlikely case where the model is perfect and the disturbance is estimated exactly, controller (14) ensures constraint satisfaction over the transient as well as asymptotic system behaviour.
- Controller (14) does not wind-up and exhibits less overshoots and aggressiveness than controller (4).

6. ILLUSTRATIVE EXAMPLE

A 2-state MIMO example is presented here. The problem is concerned with deriving the explicit tracking control law for an evaporator process studied in a sequence of works starting from (Newell and Lee, 1989). The constraints and the

nominal values of the system outputs are: $C_2^n = 25\%$, $25\% \leq C_2 \leq 30\%$, $P_2^n = 50.57KPa$, $40KPa \leq P_2 \leq 80KPa$. Similarly for the control inputs: $P_{100}^n = 193.37KPa$, $0KPa \leq P_{100} \leq 400KPa$, $F_{200}^n = 207.52kg/min$, $0 \leq F_{200} \leq 400kg/min$. Two parametric tracking controllers are designed ($\Delta t = 1$ min, $N = 3$) following the procedure described in sections 3 and 4. The controller with integral penalty is partitioned to 97 critical regions for a wide range of variations of the pure and integral states. For example in the region defined by the following set of inequalities:

$$4.5 \leq 0.2C_2 \leq 6$$

⋮

$$1.210 \cdot 10^5 \leq 4.887 \cdot 10^3 + 0.3296P_2 + 4.8868$$

The control functions are the following:

$$P_{100} = -16.575C_2 + 3.8956P_2 + 414.18;$$

$$F_{200} = -97.842C_2 + 675.86P_2 - 0.63C_{2q} + 45.63P_{2q} - 3.149 \cdot 10^4$$

The control law consists of the assembly of these control functions. Note that the prescribed function of the first control variable P_{100} is not affected at all by the integral states. The reason is that when the states lie on that region the system operates in the neighborhood or on the boundary of the constraint $C_2 \geq 25\%$. Thus, the control variable P_{100} that largely affects C_2 is readjusted to ensure constraint satisfaction and does not feature target tracking capabilities. Whereas, when the states enter the region where none of the constraints is active the control activity features integral action and the corresponding expressions are:

$$P_{100} = -3.11 \cdot 10^1 C_2 + 3.89P_2 - 1.45 \cdot 10^1 C_{2q} + 7.75 \cdot 10^2$$

$$F_{200} = -1.72 \cdot 10^2 C_2 + 6.75 \cdot 10^2 P_2 - 7.56 \cdot 10^1 C_{2q}$$

$$+ 1.45 \cdot 10^2 P_{2q} - 2.96 \cdot 10^4$$

Thus, the values of the integral coefficients in the control functions are alternating according to how close the constraints are to saturation. This characteristic clearly manifests, therein, the *anti-windup* properties of our proposed tracking controller. The tracking parametric controller with the disturbance estimator is derived in a similar fashion.

The execution of the tracking controllers is compared with the nominal controller. The system is initially perturbed to $C_{2,t=0} = 26\%$ and $P_{2,t=0} = 51.57KPa$ and as it is driven back to the origin a sequence of non-vanishing persistent step disturbances in C_1, F_1 occur. The disturbances have overall a magnitude of $\Delta F_1 \simeq \pm 0.16kg/min$ and

$\Delta C_1 \simeq \pm 0.4\%$. The profiles of disturbance F_1 and of output C_2 corresponding to the action of the nominal parametric controller (nominal parco), the tracking parametric controller with integral penalty and with estimator (tracking parco / integral, tracking parco / estimator) are displayed in Figure 1. A Kalman Filter estimator is used for the simulation of the corresponding tracking controller and its estimation of disturbance F_1 is also shown in Figure 1. The nominal controller exhibits severe constraint violations since $C_2(t) < 25\%$. The tracking controllers however, respect the constraints over the complete envelope of operation because they bring the system into the interior of the feasible region after every disturbance step.

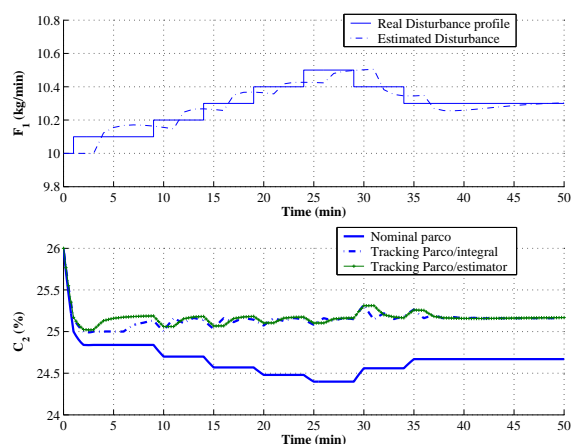


Fig. 1. Output and control profiles for nominal and tracking parametric controller

7. CONCLUSIONS

In this paper a novel framework is presented for designing model-based tracking parametric controllers for linear dynamic systems that are subject to input disturbances and uncertainties. Two control schemes are developed that consist of piecewise affine expressions for the control variables in terms of the states. The implementation of the control action is achieved by simple linear function evaluations, thus avoiding any expensive on-line computations. The controller guarantees effectively disturbance attenuation and offset elimination.

8. REFERENCES

- Bemporad, A., A.R. Teel and L. Zaccarian (2002a). l_2 anti-windup via receding horizon optimal control. In: *American Control Conference*. Anchorage, Alaska.
- Bemporad, A., M. Morari, V. Dua and E.N. Pistikopoulos (2002b). The explicit linear quadratic regulator for constrained systems. *Automatica* **38**(1), 3–20.
- Chmielewski, D. and V. Manousiouthakis (1996). On constrained infinite-time linear quadratic optimal control. *Systems & Control Letters* **29**, 121–129.
- Dua, V., N.A. Bozinis and E.N. Pistikopoulos (2002). A multiparametric programming approach for mixed integer and quadratic engineering problems. *Comp. Chem. Eng.* **26**(4–5), 715–733.
- Kothare, M.V., P.J. Campo, M. Morari and C.N. Nett (1994). A unified framework for the study of anti-windup designs. *Automatica* **30**(12), 1869–1883.
- Lee, J.H. and B. Cooley (1997). Recent advances in model predictive control and other related areas. In: *Proc. of Chemical Process Control - V: assessment and new directions for research* (J.C. Kantor, C.E. Garcia and B. Carnahan, Eds.). AIChE. pp. 201–216.
- Muske, K.R. and J.B. Rawlings (1993). Model predictive control with linear models. *AIChE J.* **39**(2), 262–287.
- Muske, K.R. and T.A. Badgwell (2002). Disturbance modeling for offset-free linear model predictive control. *J. of Proc. Control* **12**, 617–632.
- Newell, R.B. and P.L. Lee (1989). *Applied Process Control - A Case Study*. Prentice-Hall, Sydney.
- Pistikopoulos, E.N., V. Dua, N.A. Bozinis, A. Bemporad and M. Morari (2002). On-line optimization via off-line parametric optimization tools. *Comput. Chem. Eng.* **26**(2), 175–185.
- Rawlings, J.B. (2000). Tutorial overview of model predictive control. *IEEE Control Systems Magazine* **20**(3), 38–52.
- Rawlings, J.B. and K.R. Muske (1993). The stability of constrained receding horizon control. *IEEE Trans. Automatic Contr.* **38**(10), 1512–1516.
- Sakizlis, V., J.D. Perkins and E.N. Pistikopoulos (2002). *Recent Developments in Optimization and Control in Chem. Eng.*. Chap. Multiparametric Dynamic Optimization of Linear Quadratic Optimal Control Problems: Theory and Applications, pp. 195–216. Editor: R. Luus, Research Signpost, Kerala, India.
- Seborg, D.E., T. F. Edgar and D.A. Mellichamp (1989). *Process Dynamics and Control*. Wiley and Sons.
- Stengel, R.F. (1994). *Optimal Control and Estimation*. Dover Publications. Mineola, New York.
- Vogel, E.F. and J.J. Downs (2002). Industrial experience with state-space model predictive control. In: *CPC-VI Proceedings* (J. Rawlings, T. Ogunnaike and J. Eaton, Eds.). Vol. 98 of *AIChE Symposium Series*. AIChE. pp. 438–442.

DISCRETE CONTROL OF NEARLY INTEGRABLE TWO-DIMENSIONAL CONTINUOUS SYSTEMS

Stéphane Blouin ^{*,1} Martin Guay ^{*} Karen Rudie ^{**}

^{*} *Chemical Engineering, Queen's University, Canada*

^{**} *Electrical and Computer Engineering, Queen's
University, Canada*

Abstract: Many manufacturing processes involve an interplay of logical and continuous objectives. Hybrid Control Systems are well-suited for studying interactions between continuous and logical control goals. Here, a technique for generating the interfaces of a family of Hybrid Control Systems is presented. This amounts to extracting (untimed and specification-independent) abstractions for a class of nonlinear continuous systems satisfying an integrability property. A two-dimensional example illustrates an extension of the technique to a larger class of systems.

Keywords: Nonlinear systems, geometric properties, hierarchical control, state-space methods, system analysis.

1. INTRODUCTION

A Hybrid Control System (HCS) consists of a discrete-event controller for a continuous plant as illustrated in Figure 1. The y/s_i interface converts the plant output y into a controller symbolic input s_i , and the s_o/u interface transforms the controller symbolic output s_o into the plant input u .

Two distinct problems arise with HCSs. The first problem focuses on control issues in the presence of known interfaces. The second problem amounts to developing the interfaces. Herein emphasis is put on the second problem in the presence of the following situations: (i) the process has an actuation taking discrete values (“On”, “Off”, etc.), and (ii) the process has specifications of the type “if tank #1 overflows, then close valve #2”. Notice that such a setup still allows continuous control objectives.

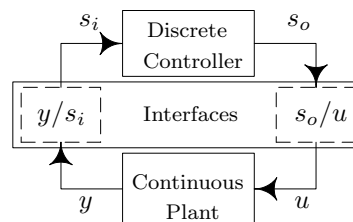


Fig. 1. Hybrid Control System

2. MOTIVATIONS

The interfaces of an HCS can be obtained by generating a finite-state machine (FSM) abstraction of the continuous system. Abstractions can be tailored to a specification (called *s-abstractions*) or independent of specifications (simply called *abstractions*). We favor abstractions because continuous control tasks are not easily expressible in terms of s-abstractions. An example of stabilization with abstractions is given in (Lunze, 1995).

The abstraction technique presented in (Lunze *et al.*, 1999) applies to linear systems. The approach presented in (Raisch, 2000) requires discrete-time

¹ Supported by the Natural Sciences and Engineering Research Council of Canada (NSERC), Fonds pour la formation de chercheurs et l'aide à la recherche (FCAR) and Ontario Graduate Scholarships (OGS).

(linear or linearized) models. Since linearization can destroy controllability (Isidori, 1995), abstractions based on a linearized model may possess fewer control capabilities than the original system. Among the approaches applying to nonlinear systems and concerned with s-abstractions, (Broucke, 1998) and (Stiver *et al.*, 2001) use the notion of dynamical invariants whereas other approaches are proposed in (Zhao, 1994) (Stursberg *et al.*, 2000). Even though nonlinear systems are considered in (Caines and Lemch, 1998), no abstraction technique is proposed. In summary, there exists no systematic technique for generating abstractions of nonlinear systems.

3. BACKGROUND

The continuous plant is modelled by

$$\dot{x}(t) = f(x(t), u(t)), y(t) = x(t), t \in \mathbb{R}_{\geq 0} \quad (1)$$

where $x(t) \in D$, $u(t) \in U$, and $y(t)$, represent a coordinate function, an input map, and an output function, respectively. The vector field f is defined on D , a connected subset of \mathbb{R}^n , and it is assumed to be analytic in x , C^1 in u and complete (Isidori, 1995). The set of input values $U = \Sigma$ is known *a priori* and

$$\Sigma := \{\sigma_k := (\sigma_k^1, \dots, \sigma_k^m) \in \mathbb{R}^m\}_{k \in \mathcal{I}_\Sigma}, \quad (2)$$

with $\mathcal{I}_\Sigma \subset \mathbb{N}$ the index set of Σ and m the number of inputs involved. The map $u : \mathbb{R}_{\geq 0} \rightarrow \Sigma$ generates piecewise-constant (from the right) input signals, which we write $u(\cdot) \in \mathcal{U}_d \subset \mathcal{U}$ with \mathcal{U} the class of admissible controls (Isidori, 1995). The *flow* of the vector field $f(\cdot, \sigma_k)$ is a mapping $\phi_k : I \times D \rightarrow D$ satisfying $\phi_k(t=0, p) = p$ for any $p \in D$ and $\partial \phi_k(t, x) / \partial t = f(\phi_k(t, x), \sigma_k)$, for each $t \in I \subset \mathbb{R}$ where I is a time interval. We denote by $\phi_k^*(I_a, \cdot)$ the flow over the time interval I_a .

Definition 1. (First Integral). Let $f : D \rightarrow \mathbb{R}^n$ be a vector field. A C^k ($k \geq 1$) real-valued function $\gamma : D' \rightarrow \mathbb{R}$ defined on D' , an open subset of D , is said to be a time-independent C^k *first integral* for the vector field f on D' if it satisfies

$$d\gamma(x) \cdot f(x)|_{x=p} = 0, \quad (3)$$

for all $p \in D'$ with $d := [\partial/\partial x_1, \dots, \partial/\partial x_n]$. \diamond

Namely, a first integral is a function whose tangent space is parallel to f everywhere in D' . There exists no generic procedure for extracting the first integrals of a nonlinear continuous system, in general (Goriely, 2001). For vector fields as in (1), a “first integral” means a non-trivial first integral ($d\gamma(x, u)|_{x=p} = 0$ only for some $p \in D'$) that is analytic in x , C^k in u with $k \geq 1$, and defined for

any set $\Sigma \subset \mathbb{R}^m$. For the following definition, we require the $n + m$ dimensional space $D'_\sigma = D' \times (\sigma - \epsilon, \sigma + \epsilon)$, where $\sigma \in \Sigma$ and $\epsilon \in \mathbb{R}^m \setminus \{0\}$ is a vector whose norm can be made arbitrarily small.

Definition 2. (Near Integrability). A system characterized by (1) and with an input map $u(\cdot) \in \mathcal{U}_d$ is *nearly integrable* over D' if for any input value $\sigma \in \Sigma$ there exist a vector $\epsilon \in \mathbb{R}^m \setminus \{0\}$ and $n - 1$ first integrals $\gamma_j(\cdot, \sigma)$, $j \in \{1, \dots, n - 1\}$, satisfying the condition

$$\text{rank}([d\gamma_1(x, \sigma), \dots, d\gamma_{n-1}(x, \sigma)]^T) = n - 1 \quad (4)$$

on an open and dense subset of D'_σ . \diamond

Definition 3. (ICSS). A system satisfying the property of Definition 2 is an *Integrable Controlled Switched System* (or ICSS). \diamond

An ICSS is such that integrability (Isidori, 1995) holds on some subset of D' despite a small perturbation in the input values. A first integral $\gamma_j(\cdot, \sigma_k)$ with $\sigma_k \in \Sigma$ is now written in a compact form as γ_j^k . To the input value set Σ is associated the set of $m \times (n - 1)$ first integrals

$$\Gamma := \{\gamma_j^k \mid k \in \mathcal{I}_\Sigma, j \in \{1, \dots, n - 1\}\}. \quad (5)$$

We now present some necessary concepts from differential topology. A smooth mapping between differentiable manifolds $g : M \rightarrow N$ with a surjective derivative at p is a submersion at p . The mapping g is a *submersion* if it is a submersion for all $p \in M$. Given $c \in g(M)$, the preimage of a submersion g is the set $g^{-1}(c) := \{p \in M \mid g(p) = c\}$. A point $c \in N$, is a *regular value* of g if $dg|_p$ is surjective for all values of p such that $g(p) = c$; otherwise c is a *critical value*. The set of regular values for g is denoted by \mathcal{R}^g . A point $p \in M$ is a *critical point* if $dg|_p$ is not surjective. By Sard’s Theorem, the set $\mathcal{R}^{j,k}$ that contains regular values for $\gamma_j^k \in \Gamma$, is dense and open in \mathbb{R} . Let $\tilde{\mathcal{R}}^{j,k} \subseteq \mathcal{R}^{j,k}$ be the largest open subset of regular values that are in the image of $\gamma_j^k(D')$. Given $\sigma_k \in \Sigma$ and $\gamma_j^k \in \Gamma$,

$$L_{j,k}^c := \{p \in D' \mid \gamma_j^k(p) = c \in \tilde{\mathcal{R}}^{j,k}\} \quad (6)$$

is referred to as a *leaf* and c is called a *first integral constant* (or FIC). The partitions induced by a set of FICs are called *leaf-partitions*.

An FSM is a triple (Q, Σ, δ) where Q , Σ , and δ represent the set of discrete states, the alphabet, and the transition map, respectively. The transition map $\delta : \Sigma \times Q \rightarrow 2^Q$ provides the state transitions of an FSM under some input values. An FSM transition structure is *deterministic* if $\delta : \Sigma \times Q \rightarrow Q$, or said otherwise, if $(\forall i \in Q)(\forall \sigma \in$

$\Sigma) \# \delta(\sigma, i) = 1$ whenever $\delta(\sigma, i)$ exists, where $\#A$ stands for the cardinality of set A .

4. PROBLEM STATEMENT

For FSM abstractions, the state set Q is defined by a partition while continuous dynamics (1) determine the transition map δ . Prior to formulating the problem, we explain some phenomena characterizing the transition structure.

Any partitioning of a continuum results in subsets, called *cells*, containing an infinite number of points. A finiteness issue arises due to the infinite number of points to consider in the treatment of each cell. This represents a challenge for obtaining the transition map δ because the task must be completed in a finite number of operations.

The vector field f is *transversal* to the cell boundary ∂ if $N(\partial, x) \cdot f(x)|_{x=p} \neq 0$ for all $p \in \partial$, where $N(\partial, x)|_{x=p}$ stands for the normal to the boundary ∂ evaluated at p . Namely, the vector field f is transversal to ∂ if it is nowhere tangent to it. Given an arbitrary partition and a boundary ∂^i , a trajectory initiated at a point p and intersecting with ∂^i can be (a) tangent to ∂^i at a point, (b) transversal to ∂^i , or (c) travelling along ∂^i , as represented in Figure 2. Transversality is a nice property since it provides a clear delineation of trajectories. The presence of non-transversal trajectories is problematic because small perturbations may alter the partition cells being encountered.

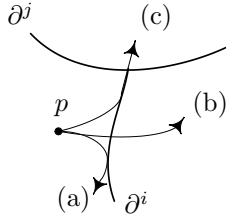


Fig. 2. Trajectory types

Given a partition cell $q_i \in Q$, the set of neighboring cells contains those cells sharing a common boundary with q_i , i.e., $N_i := \{q_{i'} \in Q \setminus \{q_i\} \mid \partial^i \cap \partial^{i'} \neq \emptyset\}$. Formally, $\mathcal{A} := (Q, \Sigma, \delta)$ is an FSM abstraction for (1) if for each pair $q_i, q_j \in Q$ and each input value $\sigma_k \in \Sigma$ satisfying $q_j \in \delta(\sigma_k, q_i)$,

- (i) $q_i = q_j$ and $(\exists p \in q_i) \phi_k(t, p) = p, \forall t \in \mathbb{R}$, or
- (ii) $q_j \in N_i$ and $(\exists p \in q_i)(\exists p' \in q_j)(\exists t \in \mathbb{R}_{>0})$ (7)
 $\phi_k^*(0, t, p) \in \bar{q}_i$ and $\phi_k(t, p) = p'$,

where \bar{q}_i denotes the set closure of q_i , i.e., $\bar{q}_i := q_i \cup \partial^i$. Thus a transition induced by σ_k from q_i to q_j exists if (i) there is an equilibrium point in q_i , or (ii) for at least one point $p \in q_i$ there is a (positive time) trajectory leading to a point $p' \in q_j$.

Consistency is a property that ensures that a sequence of transitions in the abstraction has at

least one corresponding trajectory in the underlying continuous system (Kokar, 1995) (Stursberg *et al.*, 2000). As shown in (Lunze *et al.*, 1999), consistency has strong ties with the existence of deterministic transition structures. Moreover, in (Blouin *et al.*, 2003) the authors demonstrated that the lack of transversality may induce non-deterministic transitions.

We are interested in finding, in a finite number of steps, a consistent FSM abstraction \mathcal{A} for (1). Due to space limitations, only transversality is treated.

5. TRANSVERSALITY

Given a leaf-partition, a boundary ∂^i reduces to a subset of a leaf, i.e., $\partial^i \subseteq L_{j,k}^c$ for some $k \in \mathcal{I}_\Sigma$, and $c \in \tilde{\mathcal{R}}^{j,k}$. By definition a first integral $\gamma_j^k \in \Gamma$ satisfies $d\gamma_j^k(x) \cdot f(x, \sigma_k)|_{x=p} = 0$ for all $p \in D'$. Thus a trajectory initiated on ∂^i travels along the leaf $L_{j,k}^c$ as long as σ_k remains active (case (c) of Figure 2). With two input values $\sigma_k, \sigma_{k'} \in \Sigma$, $\sigma_k \neq \sigma_{k'}$ the characterization of nontransversality is performed by using

$$d\gamma_j^k(x) \cdot f(x, \sigma_{k'}) = \psi_{j,k,k'}(x), \quad (8)$$

where the analyticity of the real-valued function $\psi_{j,k,k'}$ follows from that of γ_j^k and $f(\cdot, \sigma_{k'})$. In the presence of leaf-partitions, equation (8) detects the transversality for the whole family of leaves and flows generated by input values σ_k and $\sigma_{k'}$, respectively. Thus the characterization of the trajectory (a) in Figure 2 corresponds to points $p \in D'$ where $\psi_{j,k,k'}(x)|_{x=p} = 0$, whereas the trajectory (b) coincides with $\psi_{j,k,k'}(x)|_{x=p} \neq 0$. If $\psi_{j,k,k'}$ is a submersion, then $\psi_{j,k,k'}^{-1}(0)$ is referred to as a *non-transversality submanifold* (NTSM). Whenever a leaf $L_{j,k}^c$ does not intersect with a critical point of $\psi_{j,k,k'}$ and if the NTSM exists, then the NTSM divides the leaf in two regions $R_1, R_2 \subset L_{j,k}^c$, such that $R_1 \cap R_2 = \emptyset$, $\bar{R}_1 \cup \bar{R}_2 = L_{j,k}^c$ and $d\gamma_j^k(x) \cdot f(\sigma_{k'}, x)|_{x=p \in R_1} < 0$, and $d\gamma_j^k(x) \cdot f(\sigma_{k'}, x)|_{x=p \in R_2} > 0$. Namely, in one region the flow goes in one direction with respect to the normal $d\gamma_j^k$ while for the other region it circulates in the opposite direction.

Let us identify the set of critical points of $\psi_{j,k,k'}$ in D' with $\mathcal{C}_{j,k,k'}^p \subseteq D'$. Given the set Σ let

$$\mathcal{C}_{j,k}^p := \bigcup_{\sigma_{k'} \in \Sigma \setminus \{\sigma_k\}} \mathcal{C}_{j,k,k'}^p \subseteq D' \quad (9)$$

represent the set of all critical points in D' for the transversality of the flows generated by input values in Σ with respect to the j th leaf induced by the input value $\sigma_k \in \Sigma$. The task of characterizing non-transversal intersections is facilitated if no leaf induced by γ_j^k meets with $\mathcal{C}_{j,k}^p$.

Proposition 1

Let $\gamma_j^k \in \Gamma$ be a first integral and let $\sigma'_k \in \Sigma \setminus \{\sigma_k\}$ be arbitrary. For each point $p \in L_{j,k}^c \subset D' \setminus C_{j,k}^p$ such that $\psi_{j,k,k'}(x)|_{x=p} = 0$, the set $\psi_{j,k,k'}^{-1}(0)$ forms a submanifold of D' containing p .

Let $C_{j,k}^v := \{p \in \tilde{\mathcal{R}}^{j,k} \mid \gamma_j^k(a) = p, a \in C_{j,k}^p\}$ be the set of critical values for the transversality test and let $\hat{\mathcal{R}}^{j,k} = \tilde{\mathcal{R}}^{j,k} \setminus C_{j,k}^v$. Under certain conditions on $\hat{\mathcal{R}}^{j,k}$ and on the ICSS it can be shown that there exist approximate (possibly exact) leaf-partitions with well-characterized transversality. This is in part due to near integrability and the fact that under a small perturbation $\Delta u \neq 0$ in the input value u the transversality with input value $u' := u + \Delta u$ can be investigated.

6. BOUNDED LEAF-PARTITIONS

So far, we have assumed that the cells of a leaf-partition were bounded. Even though a visual inspection is possible for systems in $\mathbb{R}^{n=2}$, the task of verifying this assumption becomes extremely complex when $n > 2$. This section investigates when a leaf-partition generated from first integrals taken in $\hat{\Gamma} \subseteq \Gamma$ has all its cells bounded by leaves.

A nonempty open set $P \subset D'$ is *L-bounded* if there exists “a closed box made out of leaves” bounding P . An *L-partition* is a leaf-partition for which each cell is L-bounded. One can interpret L-boundedness as a homogeneity requirement among the cells of a leaf-partition.

Definition 4. (L^ϵ -boundedness). Given an open set $P \subset D'$, a point $p \in P$ is *L $^\epsilon$ -bounded* if there exist a neighborhood of p , $N_p \subset P$, and an open subset of N_p containing p and whose boundary is made of leaves.

Let A be a set and define its closure as $\bar{A} = A \cup \partial A$ with ∂A the boundary points of A . A *boundary point* $p \in \partial A$ is a point whose neighborhoods contain a point in A and a point in A^c , the complement of A . An *internal boundary point*, $p \in \partial_{int} A$, is a boundary point of A for which any neighborhood N_p satisfies $N_p \subset \bar{A}$. The external boundary $\partial_{ext} A$ complements $\partial_{int} A$ in ∂A .

Proposition 2

Let R_a and R_b be two open, distinct, and nonempty intersecting L-bounded sets with bounding boxes made out of leaves $B_a = \partial R_a$ and $B_b = \partial R_b$, respectively. Then $R_a \cup R_b \cup \partial_{int}(R_a \cup R_b)$ is a L-bounded set.

Proof: (Blouin *et al.*, 2003).□

Partition cells normally form a collection of adjacent L-bounded sets. The above result implies

that any adjacent L-bounded cells can be “glued” together to form a larger L-bounded cell. This construct enables one to link L^ϵ -boundedness to L-boundedness in the following manner.

Lemma 1. Consider an ICSS with a set of first integrals $\hat{\Gamma} \subseteq \Gamma$ as well as an open set $P \subset D'$. If each point $p \in P$ is L^ϵ -bounded, then there exists a connected and nonempty open subset $P' \subset P$ that is L-bounded.

Proof: (Blouin *et al.*, 2003).□

Lemma 1 provides a sufficient condition for the L-boundedness of a subset of D' that relies on the notion of L^ϵ -boundedness. A sufficient condition for L^ϵ -boundedness at a point is to encounter a leaf while travelling from that point in all possible directions. Rather than testing all directions, one can exploit the information about the non-transversality of a set of leaves. Given a set of first integrals $\hat{\Gamma} \subseteq \Gamma$, the set of points in D' where nontransversality occurs is

$$\Omega(\hat{\Gamma}) := \{p \in D' \mid \text{rank}(d\hat{\Gamma}(x)|_{x=p}) < n\}, \quad (10)$$

where $\text{rank}(d\hat{\Gamma}(x)|_{x=p})$ stands for the rank of the codistribution formed by the differential of all first integrals in $\hat{\Gamma}$. Thus $\Omega(\hat{\Gamma})$ forms a closed set of measure zero, which may fail to be convex (Sussman, 1973). The tangent cone to $\Omega(\hat{\Gamma})$ at a point p in $\Omega(\hat{\Gamma})$ is given by

$$C_{\Omega(\hat{\Gamma})}(p) := \{v \in \mathbb{R}^n \mid d_{\Omega(\hat{\Gamma})}^0(p, v) = 0\}, \quad (11)$$

where $d_{\Omega(\hat{\Gamma})}^0(p, v)$ is the *generalized directional derivative* of $d_{\Omega(\hat{\Gamma})}(p)$, the distance function from a point $p \in D'$ to the set $\Omega(\hat{\Gamma})$ (Clarke, 1990).

Lemma 2. Consider an ICSS with a set of first integrals $\hat{\Gamma} \subseteq \Gamma$ and its set of nontransversality points $\Omega(\hat{\Gamma})$. Let P be an open subset of D' . A point $p \in P$ is L^ϵ -bounded if $p \notin \Omega(\hat{\Gamma})$ or $p \in \Omega(\hat{\Gamma})$ and for any nonzero vector $v \in C_{\Omega(\hat{\Gamma})}(p)$, there exists a first integral $\gamma_j^k \in \hat{\Gamma}$ such that

$$d\gamma_j^k(x) \cdot v|_{x=p} \neq 0. \quad (12)$$

Proof: (Blouin *et al.*, 2003).□

Lemma 2 requires that $C_{\Omega(\hat{\Gamma})}$ is everywhere transversal to some leaf induced by the first integrals of $\hat{\Gamma}$. As (12) involves the differential of first integrals in $\hat{\Gamma}$, it does not depend on FICs, and is, therefore, invariant to further refinements or aggregations of the partition. In (Blouin *et al.*, 2003), various examples show how the L^ϵ -boundedness property is affected by the set of first integrals constituting $\hat{\Gamma}$, the set of input values Σ , and the selection of P .

Theorem 6.1

Consider an ICSS with the set of first integrals $\hat{\Gamma} \subseteq \Gamma$ and its set of nontransversality points $\Omega(\hat{\Gamma})$. Let $P \subseteq D'$ be an open set. If the conditions of Lemma 2 hold for all $p \in P$ then there exists a nonempty L -bounded connected subset $P' \subset P$. \diamond

Proof: By Lemma 1 and Lemma 2. \square

As L^ϵ -boundedness characterizes the family of leaves induced by $\hat{\Gamma}$, Theorem 6.1 provides insight into the existence of L -partitions.

7. DISCUSSION

The material presented so far holds for systems of arbitrary dimension n . In (Blouin *et al.*, 2003) it was shown that $n = 2$ represents a special case of the theory. An algorithm providing, in finite steps, the leaf-partition and the corresponding FSM abstraction of two-dimensional systems was developed. In what follows, the theory is extended to non-integrable systems evolving in $D \subseteq \mathbb{R}^2$.

In practice many chemical processes do not have known first integrals. In this category one finds nonisothermal continuous stirred-tank reactors (CSTR). An instance of a two-dimensional model involving a first-order irreversible reaction $A \rightarrow B$ with constant hold-up is given by

$$\begin{aligned} \frac{dC}{dt} &= -DC - k_0 e^{(-E/RT)} C + DC_{in} \\ \frac{dT}{dt} &= -DT + \beta k_0 e^{(-E/RT)} C + DT_{in} - u \end{aligned} \quad (13)$$

where C (mol/L) and T ($^\circ C$) represent the concentration of A and the temperature of the mixture, respectively (Ogunnaike and Ray, 1994). The input u corresponds to the heat transferred through the coil. The following parameters are used: $k_0 = 1.287e+12$, $E/R = 9758.3$, $\beta = 1.4936$, $D = 14.19 h^{-1}$, $C_{in} = 0.5$ and $T_{in} = 100$.

For two-dimensional systems modeled by $dx_1/dt = f_1(x_1, x_2)$ and $dx_2/dt = f_2(x_1, x_2)$, the corresponding one-form is $\omega = \omega_1 d(x_1) + \omega_2 d(x_2) = f_2 d(x_1) - f_1 d(x_2)$. Any function V satisfying $dV = \omega$ is a first integral. An approximate first integral \hat{V} is such that $d\hat{V} - \omega = \epsilon$ with ϵ an error term. If \hat{V} is expressed as $\hat{V} = \sum_{i=1}^k a_i \phi_i(x_1, x_2)$, where ϕ_i 's represent approximating functions, then the identification of the weight vector $a = [a_1, \dots, a_k]$ can be performed by solving

$$\int_{\Theta} \sum_{j=1}^n \left(\omega_j - \sum_{i=1}^k a_i \frac{\partial \phi_i}{\partial x_j} \right) \frac{\partial \phi_h}{\partial x_j} d\Theta = 0, \quad (14)$$

for $h = 1, \dots, k$ over a domain Θ . Thus one gets $A a^T = b$ where

$$b = \begin{bmatrix} \beta^1 \\ \vdots \\ \beta^k \end{bmatrix}, \quad A = \begin{bmatrix} \alpha_1^1 & \dots & \alpha_k^1 \\ \vdots & & \vdots \\ \alpha_k^1 & \dots & \alpha_k^k \end{bmatrix}, \quad (15)$$

with

$$\begin{aligned} \alpha_i^h &= \int_{\Theta} \left(\frac{\partial \phi_i}{\partial x_1} \frac{\partial \phi_h}{\partial x_1} + \frac{\partial \phi_i}{\partial x_2} \frac{\partial \phi_h}{\partial x_2} \right) d\Theta \\ \beta^h &= \int_{\Theta} \left(f_2 \frac{\partial \phi_h}{\partial x_1} - f_1 \frac{\partial \phi_h}{\partial x_2} \right) d\Theta \end{aligned} \quad (16)$$

as $\omega_1 = f_2$ and $\omega_2 = -f_1$. Here, Θ is a region defined to be $[C_l, C_h] \times [T_l, T_h]$ with $C_l = 0.3$, $C_h = 0.65$, $T_l = 350$ and $T_h = 450$. Figure 3 shows trajectories of (13) induced by the input value set $\Sigma := \{-5000, 5000\}$ over Θ . The ϕ_i 's are elements of a polynomial of order r . Thus $i = 1, \dots, r^2$ and

$$\hat{V} = \sum_{a=1}^r \sum_{b=1}^r a_i \phi_i, \quad \text{with } \phi_i = C^a T^b. \quad (17)$$

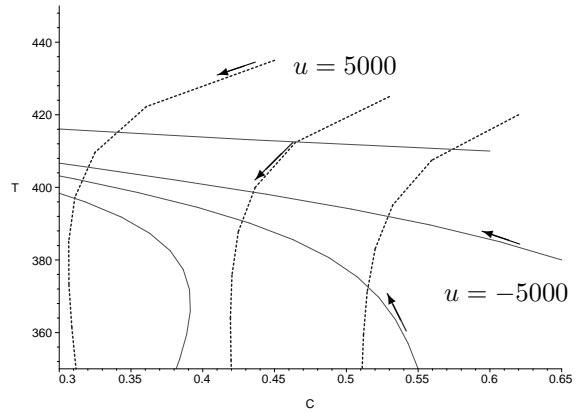


Fig. 3. Trajectories over Θ for $u \in \Sigma$.

In Figure 4, some approximate first integrals \hat{V} for $u \in \Sigma$ are shown. The FICs for $u = -5000$ and $u = 5000$ are $(-2500, -1200, -500, 100, 500, 800)$ and $(3200, 3800, 4400, 5000)$, respectively. The circled integers are labels for the L -bounded cells of the leaf-partition. That is, the FSM abstraction has the state set $Q := \{1, 2, 3, 4, 5, 6, 7, 8, 9, 10\}$. Polynomials of order 5 and 3 were used for $u = -5000$ and $u = 5000$, respectively. The corresponding FSM abstraction is presented in Figure 5. The transition structure of this FSM abstraction is deterministic because at each state an input value induces a unique transition. Transitions marked by an “ \times ” are disabled because they lead outside the set of L -bounded cells.

Even though the FSM abstraction was obtained in an *ad hoc* manner, the algorithm could be modified so that the abstractions are obtained systematically from exact or approximate first integrals. In the above example the selection of a smaller region Θ or the choice of some other ϕ_i 's

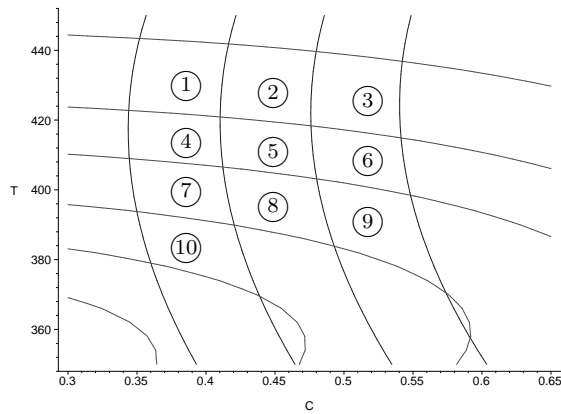


Fig. 4. Approximate leaf-partition.

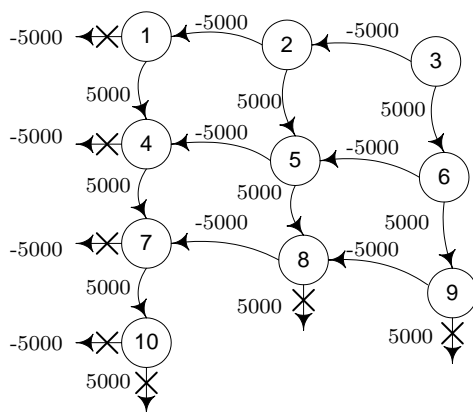


Fig. 5. Approximate FSM abstraction

could provide a better fit between the trajectories and the approximate first integrals.

An extension of the algorithmic procedure to handle higher-dimensional systems is the topic of future research.

REFERENCES

- Blouin, S., M. Guay and K. Rudie (2003). Discrete Abstractions for Nearly Integrable Continuous Systems: The Two-dimensional Case. To appear in *International Journal of Hybrid Systems*.
- Broucke, M. (1998). A Geometric Approach to Bisimulation and Verification of Hybrid Systems. In: *Proceedings of the 37th IEEE Conference on Decision and Control*. pp. 4277–4282.
- Caines, P. E. and E. S. Lemch (1998). On the Global Controllability of Hamiltonian and Other Nonlinear Systems: Fountains and Recurrence. In: *Proceedings of the 37th IEEE Conference on Decision and Control*. pp. 3575–3580.
- Clarke, F. H. (1990). *Optimization and Nonsmooth Analysis*. Philadelphia, SIAM.

- Goriely, A. (2001). *Integrability and Nonintegrability of Dynamical Systems*. World Scientific.
- Isidori, A. (1995). *Nonlinear Control Systems*. Springer-Verlag, Second Edition.
- Kokar, M.M. (1995). On Consistent Symbolic Representations of General Dynamic Systems. *IEEE Transactions on Systems, Man and Cybernetics* **25**(8), 1231–1241.
- Lunze, J. (1995). Stabilization of Nonlinear Systems by Qualitative Feedback Controllers. *Int. J. Control* **62**(1), 109–128.
- Lunze, J., B. Nixdorf and J. Schroder (1999). Deterministic Discrete-event Representation of Linear Continuous-variable Systems. *Automatica* **35**, 395–406.
- Ogunnaike, B. A. and W. H. Ray (1994). *Process Dynamics, Modelling, and Control*. Oxford University Press.
- Raisch, J. (2000). Discrete Abstractions of Continuous Systems - an Input/Output Point of View. *Mathematical and Computer Modelling of Dynamical Systems*, Special issue on *Discrete Event Models of Continuous Systems* **6**(1), 6–29.
- Stiver, J. A., X. D. Koutsoukos and P. J. Antsaklis (2001). An Invariant Based Approach to the Design of Hybrid Control Systems. *International Journal of Robust and Nonlinear Control* **11**(5), 453–478.
- Stursberg, O., S. Kowalewski and S. Engell (2000). On the Generation of Timed Discrete Approximations for Continuous Systems. *Mathematical and Computer Modelling of Dynamical Systems*, Special issue on *Discrete Event Models of Continuous Systems* **6**(1), 51–70.
- Sussman, H.J. (1973). Orbits of Families of Vectors Fields and Integrability of Distributions. *Transactions of the American Mathematical Society* **180**, 171–188.
- Zhao, F. (1994). Extracting and Representing Qualitative Behaviors of Complex Systems in Phase Space. *Artificial Intelligence* **69**(1-2), 51–92.